# Chemical Preparation of Supported Bimetallic Catalysts. Gold-Based Bimetallic, a Case Study

Catherine Louis

catalysts

MDPI

Review

# Chemical Preparation of Supported Bimetallic Catalysts. Gold-Based Bimetallic, a Case Study

**Catherine Louis**

Sorbonne Universités, UPMC Univ Paris 06, CNRS UMR 7197, Laboratoire de Réactivité de Surface, 4 Place Jussieu, Paris F-75005, France; catherine.louis@upmc.fr; Tel.: +33-144-273-050

Academic Editor: John R. (JR) Regalbuto
Received: 10 May 2016; Accepted: 24 June 2016; Published: 26 July 2016

**Abstract:** This review focuses on the chemical methods used to prepare supported bimetallic heterogeneous catalysts, i.e., bimetallic nanoparticles deposited on a support. The review is limited to the preparation of gold-based bimetallic catalysts and moreover to bimetallic nanoparticles supported on powder inorganic supports, i.e., on the surface or in the porosity, and not on model supports such as single crystals.

**Keywords:** gold; bimetallic; particle; catalyst; support; preparation; colloid

## 1. Introduction

In the field of heterogeneous catalysis, which involves the use of solid materials as catalysts for gas phase reactions and also for some liquid phase reactions, metal catalysts constitute an important class of catalysts. They are involved in many types of reactions such as hydrogenation, dehydrogenation, hydrogenolysis, isomerization, oxidation, etc. They most often consist of metal particles of nanometric size supported on a support, oxide, carbons etc., so as to stabilize them and in some cases to generate bifunctional catalysts thanks to the acid-base properties of the support. For instance, bifunctional metal-acid catalysts are required for selective ring opening (increase of cetane number), hydroisomerization (increase of octane number), hydrocracking of heavy oils, reforming, and dewaxing. In the last ten years, supported bimetallic particles catalysts have shown a huge development for several reasons:

- The intrinsic properties of bimetallic particles may lead to catalytic properties different from those of the parent metals, e.g., to enhanced activity, selectivity, and/or stability;
- The recent developments of characterization techniques, especially in electron microscopy allow now to characterize the bimetallic character of the particles much more accurately, e.g., to characterize the structure and composition of individual particles, and in addition, often in conditions in situ or operando.
- The advances in catalyst preparation, especially the development of methods involving the use of colloids (Section 4) or of those based on surface reduction–oxidation reactions (Section 5.3).

Compared to monometallic catalysts, it is obvious that the elaboration, characterization, and catalytic study of bimetallic catalysts are much more complex because of:

- The variety of possible metallic couples and their various extents of miscibility;
- The variety of possible chemical compositions for a given bimetallic system and also the distribution in chemical compositions among the particles of a given sample;
- The variety of particle structures that depend on the nature of the metals and on the synthesis methods, and their possible restructuration in reaction conditions.

Most of the preparation methods of bimetallic catalysts are based on the same principles as those of monometallic ones, i.e., deposition of metal precursors onto a support from aqueous phase, followed by thermal or chemical reduction to produce supported metal NPs (also called deposition-reduction) or pre-synthesis of metal nanoparticles in a liquid phase (also called sol or colloids) by chemical reduction of a metal precursor in the presence of stabilizing agents, followed by deposition onto a support (also called reduction-deposition). Specific preparation methods have also been developed for the synthesis of supported bimetallic particles.

This review focuses on these chemical methods used to prepare supported bimetallic nanoparticles (NPs), but is limited to the preparation of bimetallic-gold NPs supported on powder inorganic supports (no model supports). One reason for the choice of gold is that this is the most recent metal studied as a catalyst after Haruta's discovery in 1987 that oxide-supported gold nanoparticles were exceptionally active in CO oxidation at room temperature [1,2]. In addition, gold is a "challenging" catalytic metal because the particles must be small to be active, in general smaller than 5 nm, to increase the proportion of low coordination surface sites (edges and corners), which are the active sites.

Gold-based bimetallic catalysts are also very interesting systems. In oxidation reactions, gold supported on oxides is the best catalyst to run the reaction of CO oxidation at RT with a high activity [3–6]. To improve its stability, attempts have been made to combine gold with a second metal, for instance, Ag, which is also more prone to activate $O_2$ [7–9]. Gold-based bimetallic catalysts are also currently studied in selective oxidation of molecules such as benzyl alcohol or other ones arising from biomass (often AuPd catalysts). Gold is not very active as a hydrogenation catalyst because of its low ability to activate $H_2$, but it turns out that it is highly selective to semi-hydrogenation; to improve activity, a second metal can be added [10–12]. For more details on the reactions of interest with gold-based bimetallic catalysts, the reader can refer to the titles of the papers cited in the reference section.

A rather large number of metals has been coupled with gold and investigated as catalysts. Some of them, such as Pd, Cu, and Ag, are miscible with gold in a large range of compositions while others are only partially miscible or immiscible (Ni, Ru, Pt, Co, Fe). In this case, the preparation of bimetallic nanoparticles is more challenging.

Regarding the characterization of the bimetallic nanoparticles, many techniques can be used, from classical and simple ones, such as X-ray diffraction (XRD), that can provide an overall rough view of the bimetallic character provided that the particles are large enough and that the lattice parameters of the two metals are different enough, to more sophisticated techniques, such as X-ray photoelectron spectroscopy (XPS) thanks to binding energy (BE) shifts that may attest for charge transfer between two metals, UV-visible spectroscopy able to show possible shifts and shape changes of the gold plasmon band, IR spectroscopy coupled with the adsorption of CO as probe molecules (CO-FTIR and CO-DRIFTS), and X-ray absorption fine structure spectroscopy (XAFS); some catalytic reactions can also be used to characterize indirectly the samples. All these techniques provide an overview of the bimetallic character of the nanoparticles, but the various techniques of electron microscopy with aberration corrections, high resolution transmission electron microscopy (HRTEM) or scanning transmission electron microscopy (STEM), energy-dispersive X-ray spectroscopy (EDX or EDS), high angle annular dark field imaging (HAADF) and electron energy loss spectroscopy (EELS), can now bring information on individual particles, not only in ultra high vacuum (UHV) but also under controlled atmosphere.

## 2. Deposition-Reduction (Thermal Reduction)

### *2.1. Impregnation*

Impregnation, which is no longer the most used method nowadays for the preparation of monometallic Au NPs on oxides, still remains in use for the preparation of Au-based bimetallic catalysts. They can be synthesized by co-impregnation or successive impregnations or also impregnation

associated to another method. Among the Au-based bimetallic catalysts, the one most frequently prepared by impregnation is certainly Au-Pd. Supported Au-Pd catalysts have been prepared by co-impregnation of $HAuCl_4$ and $PdCl_2$ (or $H_2PdCl_4$) on various supports, $TiO_2$ [13,14], $Al_2O_3$ [15], mesoporous silica [16], $CeO_2$ [17], Metal Organic Framework [18], activated carbon [19], and carbon nanotubes [20]. After impregnation, the samples are either calcined and reduced, or directly reduced at various temperatures. For not fully elucidated reasons, in some cases, rather good results in terms of bimetallic character and of small particle sizes are obtained [15,17,20], while in other ones, bimodal size distributions or large particle sizes are obtained [13,16,18,19]. In spite of the fact that Au and Pd are miscible in any proportion, the samples containing bimodal particle size distribution also showed heterogeneous composition; the large particles (up to 50 nm or more) were gold-rich as attested by XRD and electron microscopy, while the smaller ones were Pd-rich. Attempts were made to reduce the particle size by addition of HCl during the preparation [14] or washing with $NH_4Cl$ [21].

Co-impregnation and successive impregnation have been also used to prepare other supported bimetallics, such as Au-Cu/$SiO_2$ [22], Au-Cu/$TiO_2$ [23], Au-Ir//$SiO_2$ [24], and Au-Pt/$TiO_2$ [25,26]. Again, the resulting particle sizes are at variance, and they also depend on the Au/M ratio. For instance, Au-Cu/$TiO_2$ catalysts were prepared by co-impregnation of $HAuCl_4$ and $CuCl_2$ to achieve 4 wt % total metal loading and Au:Cu molar ratios of 3:1, 1:1 and 1:3 [23]. After reduction in $H_2$ at 400 °C, the average particle sizes were 13.5, 9.3, and 7.3 nm, respectively, and showed that the particle size decreased as the proportion of copper increased. The shift in the XRD lattice parameters and in the XPS Au binding energy, as well as EELS and HRTEM characterization performed on individual particles demonstrated the existence of Au-Cu alloy particles. In the two other systems, although Au is not miscible in Ir and Pt, small bimetallic particles were obtained. In the case of Au-Pt/$TiO_2$ [25], the particle structure was found to depend on the reduction conditions as Au core-Pt shell structures were identified after reduction at 250 °C and alloy ones after reduction at 500 °C.

### 2.2. Ion Adsorption

Ion adsorption has been barely used for the preparation of bimetallics. However, one could find an example of co-adsorption of $PdCl_2$ and $HAuCl_4$ solution performed at low pH (pH 4) for the preparation of Au-Pd on Mg-Al Layered Double Hydroxide (also called hydrotalcite) [27]. After chemical reduction in ethanol and hydrazine ($NH_2NH_2$), small particles were obtained (2.4 nm), and would be bi-metallic according to the XPS results attesting for an electron transfer between Au and Pt.

### 2.3. Deposition-Precipitation

The method probably most used for the preparation of supported bimetallics by deposition-reduction is certainly deposition-precipitation performed at fixed basic pH or under variable pH with urea (DPU), either as co-deposition-precipitation (Co-DP), or as successive deposition-precipitation. However, one must be aware that this method is not suitable for gold deposition-precipitation when the supports are oxides with a low point of zero charge (PZC <5) such as silica (PZC ~2), silica-alumina (PZC ~1) [28] or are activated carbons [29].

Co-DP was performed for the preparation of Au-Pd on $TiO_2$ with NaOH at around pH 6.5 [30]. The Au loading could not exceed 1 wt %, but Pd was quantitatively deposited (up to 0.8 wt % Pd), and after thermal treatment, bimetallic particles were observed by STEM-EDS (Figure 1) with average particle sizes of around 7 nm, i.e., larger than monometallic Au (3.4 nm) but smaller than Pd ones (11 nm). Co-DP is in principle not suitable for the preparation of supported Au-Ag (miscible) because the chlorides of the Au precursor may induce the precipitation of AgCl. However, Co-DP with $NH_3$ was successfully applied to the preparation of Au-Ag/$CeO_2$, leading to the formation of particles smaller than 3 nm, the size of which decreased as the Ag:Au ratio increased [31]. Co-DP of Au-Pt (non-miscible metals) on $TiO_2$ with NaOH at pH 9–10 led to the formation of particles of 4–5 nm after reduction; they were larger than Au or Pt monometallic particles but they were bimetallic as attested by XPS and temperature programed reduction (TPR) [26]. In the case of co-DPU of Au-Pd

on $TiO_2$ or $Al_2O_3$, it was found that Pd could not be 100% deposited in contrast with gold, in spite of low nominal Pd loadings (<0.1 wt %), but the final catalysts contained small particles (<3 nm) after reduction at 500 °C which were bimetallic (at least, no indication of the presence of monometallic Pd) according to characterizations by CO-DRIFTS, TPR and selective hydrogenation reaction [15]. However, Co-DPU of Au-Pd (1 wt %–1 wt %) was found possible on ordered mesoporous silica HMS functionalized with mercaptopropyl groups; after reduction, particles were of around 2 nm and bimetallic according to XRD and XPS [32]. Co-DPU is also an efficient technique for the co-deposition of Au-Cu ($HAuCl_4$ and $Cu(NO_3)_2$) on $TiO_2$, leading to small and bimetallic Au-Cu particles with a large range of composition [33,34].

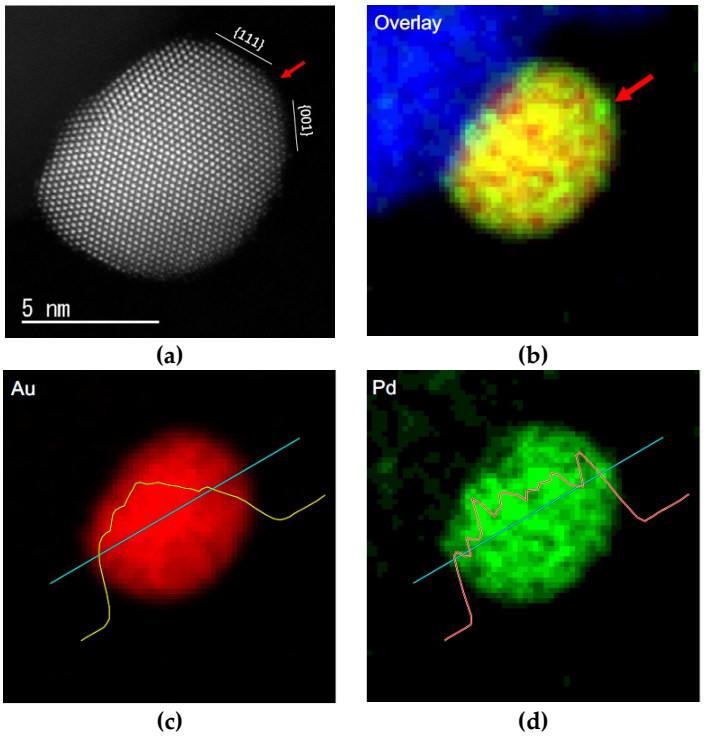


**Figure 1.** A Au-Pd nanoparticle on $TiO_2$ support (Co-DP with NaOH at pH 6.5); (**a**) High-resolution STEM (scanning transmission electron microscopy) image; (**b**,**c**,**d**) high resolution EDS analysis of the same particle—Adapted with permission from [30]. Copyright 2014, Springer.

Au-Ir/$TiO_2$ (Ir/Au = 1) catalyst (low miscibility) was prepared by sequential deposition-precipitation with urea (DPU) of Ir then Au [35]. Activation under hydrogen at 400 °C led to small metal particles (2–3 nm). Characterization by CO-DRIFTS revealed the existence of Ir-Au interactions, and XPS and TPR showed that gold hindered the re-oxidation of iridium in oxidizing atmospheres at least to some extent. Finally, the synergistic effect of the two metals observed in the reaction of propene oxidation confirmed the formation of Ir-Au bimetallic particles. Au-Ag catalysts supported on $TiO_2$ were also prepared by sequential deposition-precipitation, DP NaOH of silver first, then DPU of gold with different Au/Ag atomic ratios [8,36]. UV-visible and micro-EDS of individual particles (3–4 nm) revealed that the bimetallic character of the particles increased with the $H_2$ reduction temperature between 350 and 650 °C.

### *2.4. Combination of Preparation Methods*

One can find examples combining two different preparation methods. For instance, Au-Pd/$TiO_2$ catalysts were prepared by $PdCl_2$ impregnation (0.5 wt %) then Au deposition-precipitation (Au/Pd/$TiO_2$) and vice-versa, Au deposition-precipitation then $PdCl_2$ impregnation (Pd/Au/$TiO_2$) [37].

Their characterization study revealed the relevance of the order of the sequences of preparation. For the first sample type, the state of dispersion of Pd on $TiO_2$ changed during the loading of Au, resulting in the formation of Au-Pd alloy particles with a bimodal particle size distribution of average sizes 1.7 and 7.9 nm, and in change in the electronic properties of Pd species. In contrast, the alloy formation was not clearly detected in the second type of sample $Pd/Au/TiO_2$, and the sample contained large Au particles (30–50 nm) in addition to smaller ones of Pd (2–8 nm). $Au-Pd/CeO_2-ZrO_2$ samples were prepared by Au DP with $Na_2CO_3$ at pH 8 then after washing and calcination, by impregnation with $Pd(NO_3)_3$ followed by calcination at various temperatures [38]. Particles were around 3 nm and bimetallic according to XRD and STEM-HAADF.

$Au-Ru/CeO_2-ZrO_2$ samples (low miscibility) were prepared by Au DP with $Na_2CO_3$ at pH 8 then after washing and drying, by impregnation with $Ru(NO)(NO_3)_3$ followed by reduction at 350 °C under $H_2$ [39]. Samples with 1:0.5, 1:1, and 1:2 Au/Ru ratios were prepared, leading to small bimetallic particles from 2.7 to 3.0 nm in average as %Ru increased. Combined STEM-HAADF imaging and STEM-EDS analysis performed over individual particles revealed that the composition of the Au-Ru nanoparticles varied drastically with size; the smallest particles tended to be Ru-rich, while the largest ones were Au-rich in addition to the presence of both types of monometallic particles.

Ion adsorption was associated with impregnation. For instance, for the preparation of $Au_1-Cu_3/TiO_2$, gold anion adsorption was performed first followed by washing with ammonia then impregnation of $Cu(NO_3)_2$ [40]. After reduction at 300 °C, bimetallic particles were evidenced by HRTEM, TPR, and XPS with 3.5 nm size according to XRD.

## 3. One-Pot Deposition-Reduction (Reduction in Liquid Phase)

Up to here, thermal treatments have been mentioned to reduce supported precursors into metal particles. It is also possible to perform a chemical reduction by addition of a reducing agent in the suspension containing the powder sample. However, this requires a further step of thorough washing to eliminate all traces of the reducer. Chemical reduction can also be assisted by microwave. Alternatively, other reduction modes can be performed in the liquid phase, such as photo-reduction or sono-chemical reduction. In most cases, deposition and reduction can be performed in a single step or one-pot. The reduction mode can have an influence on the final particle size and on its composition, but in general, the extent of metal deposition is found to be almost quantitative.

### *3.1. Chemical Reduction*

A method for the preparation of bimetallic catalysts consists of the successive deposition of the first metal salt on the support and its reduction by a chemical agent followed by the same procedure for the second metal.

Liu et al. developed this type of method for the preparation of Au-Cu and Au-Ag on silica supports (amorphous and with organized mesopores SBA-15), previously functionalized with APTES (3-aminopropyl triethoxysilane) (Figure 2). A $HAuCl_4$ solution was added to APTES-SBA-15 [41] or to APTES-$SiO_2$ [42,43], followed by reduction with $NaBH_4$. After washing, the solid was immersed into an aqueous solution of copper or silver nitrate, which was then reduced by addition of $NaBH_4$. After washing and drying, the solid was calcined at 500 °C then reduced at 550 °C in $H_2$. The authors mentioned that the thermal treatment of reduction with $H_2$ was necessary for the formation of Au-Cu or Au-Ag alloy. In the case of Au-Cu, the resulting metal particle size in SBA-15 was 2.4 nm for Au:Cu = 3:1 and 2.8 nm for Au:Cu = 1:1, i.e., smaller than in the monometallic gold counterpart (5.0 nm) [41,43]. In the case of silica, the same trend was observed, i.e., Au-Cu nanoparticles were significantly smaller (3.0–3.6 nm) than in the monometallic Au ones (5.7 nm). XRD and HRTEM performed on several particles revealed that the d-spacing corresponded to that of a Au-Cu alloy. In the case of Au-Ag on SBA-15, silica and alumina, the authors insist on the fact that it was imperative to perform a thorough washing after the Au deposition-reduction, in order to remove the chlorides before the addition of $AgNO_3$ [42]. According to UV-Visible spectroscopy, HRTEM and XPS, nanoparticles of 2–3 nm with a

gold-silver alloy core and a silver nanoshell were formed in the channels of SBA-15. After the final thermal treatment of calcination and reduction in $H_2$ at 550 °C, the nanoparticles maintained their size, but they were transformed into an alloy-type structure. It is noteworthy that the bimetallic particles, Au-Cu or Au-Ag, prepared by this method were found to be highly thermally stable, since their sizes remained substantially unchanged (~3 nm) even upon calcination in air at 500 °C.

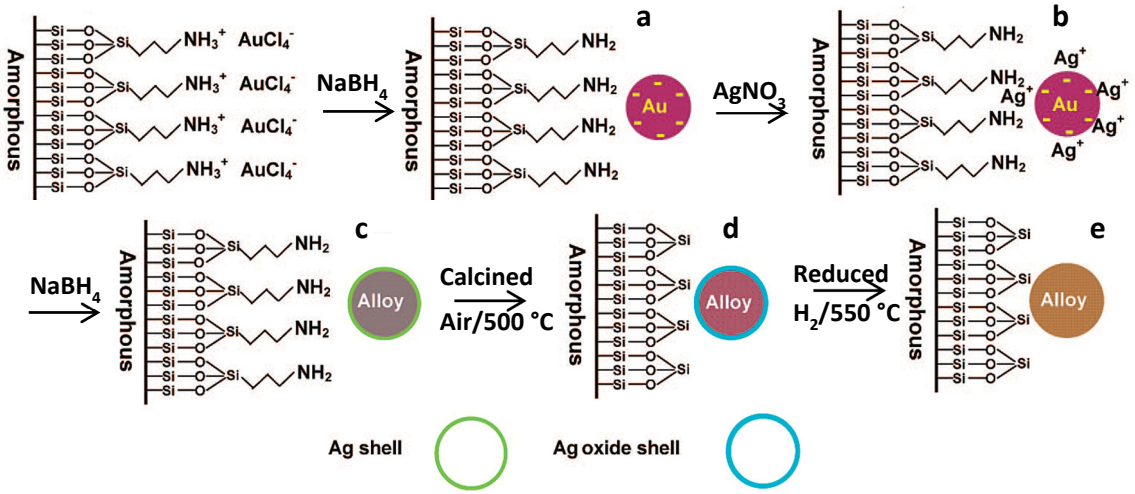


**Figure 2.** Schematic illustration of the procedure of synthesis of $SiO_2$-supported Au-Ag alloy nanoparticles. (**a**) Initially formed Au particles; (**b**) $AgNO_3$ adsorbed on the Au particles; (**c**) Au-Ag nanostructure with alloy core surrounded by a silver shell; (**d**) Au-Ag nanostructure with more gold-rich alloy core covered by a Ag oxide shell; (**e**) random alloy of Au-Ag nanoparticles on $SiO_2$ support—Adapted with permission from [42]. Copyright 2009, American Chemical Society.

Au-Pd particles were synthesized on porous germania using hydrazine as the reducing agent [44]. After three days of immersion of calcined germania nanospheres in a solution of $HAuCl_4$ in ethanol and water, hydrazine hydrate was added dropwise. Then, under $H_2$ bubbling and mixing, the color changed from pale-yellow to pink, indicating gold nanoparticle formation. Afterwards, a $H_2PdCl_4$ solution was added. The gradual color change indicated the formation of bimetallic particles, and this was confirmed by EDS, XRD, and UV-Visible spectroscopy. TEM showed that the particles were located in the porosity of germania nanospheres, with an average size of 7–10 nm.

Alternatively, Au-Cu supported on silica was prepared by the adsorption of $Au(en)_2^{3+}$ cations, followed by reduction at 150 °C then by sample immersion in a solution of copper acetate $Cu(C_2H_3O_2)_2$ into a mixture of 1-octadecene, oleic acid ,and oleylamine, under Ar [45]. After water elimination, the sample was washed with ethanol and dried. The mean particle size in AuCu (1:1)/$SiO_2$ was smaller (4 nm) than Au NPs in the Au/$SiO_2$ catalyst (4.9 nm), and EXAFS showed that the particles were bimetallic.

Co-deposition-reduction can also be performed. Au-Pd nanoparticles were prepared on phosphate-modified hydrotalcite by co-impregnation with a solution of $HAuCl_4$ and $PdCl_2$ followed by chemical reduction obtained by addition of lysine (pH 8–9) then of $NaBH_4$, washed and dried at 60 °C [46]. Nanoparticles of 4–5 nm with a d-spacing attesting the formation of Au-Pd alloy were obtained. Au-Ni (non miscible) was also prepared in a single step on activated carbon [47]. A suspension of carbon in an ethylene-glycol solution containing $HAuCl_4$ and $NiCl_2$ was heated at 85 °C then hydrazine ($NH_2NH_2$) was added, and the suspension was maintained at basic pH. However, Au-Ni alloying was obtained by heating the sample under $N_2$ at temperatures between 300 and 500 °C. Alloying improved with temperature, but particle size increased (>10 nm) and unalloyed Ni remained on the sample. However, they could be eliminated by acid treatments.

### 3.2. Photo-Deposition

Photo-deposition, co- or successive, is also a method, which allows the preparation of bimetallic catalysts in a single pot. This has been done for Au-Pt NPs in extra large three-dimensional mesoporous titania (EP-$TiO_2$) from a solution containing $HAuCl_4$, $H_2PtCl_6$ and the support dispersed in methanol solution [48]. After deoxygenation, the suspension was subjected to UV irradiation. The yield of metal deposition was 90%, and the actual composition was very close to the nominal one. The Au-Pt particles were 7.3 nm with a Au core–Pt shell structure (Figure 3a,b). After washing, drying and calcination at 350 °C, the particle size did not drastically change (7.9 nm), but the structure became homogeneous alloy (Figure 3c,d).

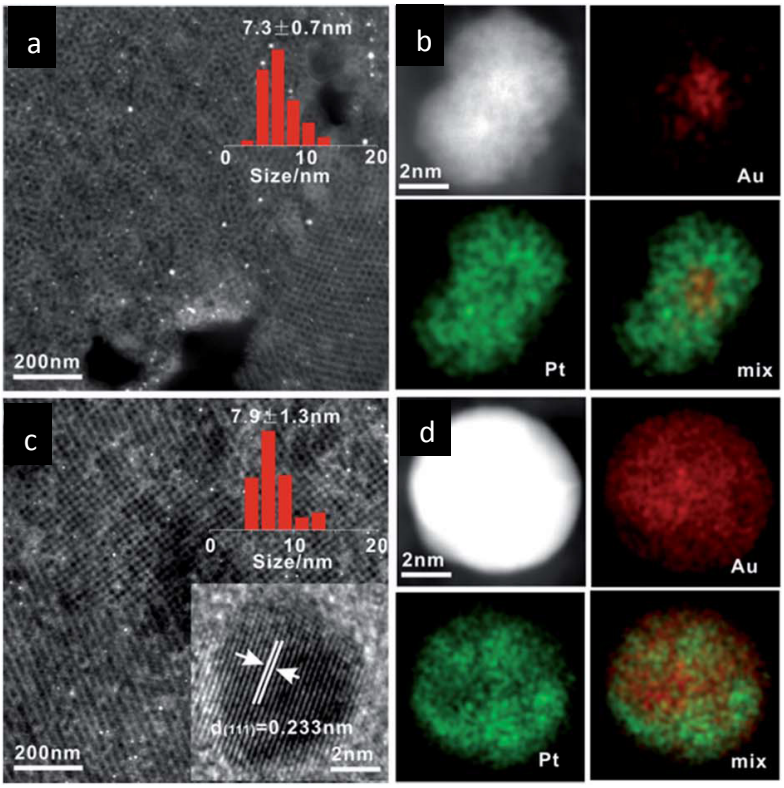


**Figure 3.** HAADF-STEM images and particle size distribution, typical EDS mappings of $Au_{50}Pt_{50}$/EP-$TiO_2$ after the photo-deposition (**a**,**b**) and after annealing at 350 °C (**c**,**d**). Adapted with permission from [48]. Copyright 2014, Royal Society Chemistry.

Successive photo-deposition has been performed for the preparation of Au-Cu/$CeO_2$. Gold was first photo-deposited according to a protocol close to the one described above, but this led to larger particles (27 nm for 0.2 wt % Au) and it was followed by Cu photo-deposition from copper sulfate precursor, leading to still larger NPs (58 nm for 0 wt % Au and 0.8 wt % Cu) [49].

### 3.3. Reduction via the Support

Supports such as graphene oxide can also play the role of reducing agent. A simple method was developed to fabricate Au-Ag nanoparticles on graphene oxide thanks to the spontaneous and simultaneous redox reactions between $AgNO_3$, $HAuCl_4$, and graphene oxide in an aqueous solution heated at 84 °C [50]. Characterization by XPS, STEM, and EDS proved that the particles were 10–20 nm and bimetallic of alloy-type with shells enriched in silver. In addition, Au-Ag alloy nanoparticles with other shapes than spherical, i.e., core-shell-like, dendrimer-like and flower-like were obtained by simply modifying the concentration of the reactants and the reaction temperature. Chen et al. [51] also

described a one-pot method to synthesize Au-Pd nanoparticles dispersed on graphene nanosheets. They were mixed first in an aqueous solution of $HAuCl_4$, then $K_2PdCl_4$ was added at RT, and bimetallic particles of 3.4 nm were obtained according to HRTEM and STEM-HAADF.

## 4. Reduction-Deposition (Deposition of Preformed Metal Nanoparticles)

The technique of deposition of metallic nanoparticles preformed in solution (colloids or sols), also called sol immobilization, is another way to prepare supported bimetallic samples. In principle, the advantage of this method is that the particle size is controlled with a narrow size distribution. Metal colloids are obtained by reduction of a metal precursor in solution in the presence of stabilizing or capping agents, which can be molecules such as CO, citrate, thiol, or amine (e.g., lysine or oleyamine), or polymers such as poly-vinylpyrrolidone (PVP), and poly-vinylalcohol (PVA). The stabilizers can also be micelles formed with diblock copolymers or surfactant, and dendrimers. The stabilizers are added to the solution to control the growth of the particles during reduction and avoid aggregation and precipitation. Reduction is usually performed by addition of a chemical agent such as those mentioned earlier, sodium borohydride, hydrazine or weaker reducing agents such as amine-borane complexes, methanol or glucose. The stabilizer may also act as a reducer, this is the case of sodium citrate and tetrakis(hydroxymethyl)phosphonium chloride (THPC). Reduction can be assisted by heating, sonication, radiolysis, UV or microwave irradiation. The formation of a gold-based bimetallic sol is attested by the color change of the solution, for instance from pale yellow or colorless to pink or red for monometallic gold. The average size and size distribution as well as the shape and the composition, strongly depend on the conditions of synthesis.

Depending on the final catalytic applications, stabilizing agents (SA) may have to be eliminated; this is the case for further gas phase catalytic reactions. In the case of liquid phase reaction, the density of SA must be controlled, and the presence of SA can even play a positive role in activity, selectivity and stability; for instance PVA-stabilized Au on $SiO_2$ showed a positive influence on the activity of glycerol oxidation and selectivity [52]. The removal of SA is a critical step because particles may sinter, and stabilizer residues may poison the catalyst [53]. Thermal treatments under air or oxygen are the most frequently used treatments. However, sintering can be prevented using a SA that decomposes at low temperature. This holds for lysine, which can decompose at 200 °C without growth of the particles (<5 nm) supported on $\alpha$-$Fe_2O_3$ [54]. Alternatively, ozone treatment or plasma activation can be used, both performed at RT. However, they require thin layers of materials, and they are rather applied to planar model catalysts. Only in a few cases, have they been used for powder supports with monometallic gold particles: the removal of thiolate phosphine ligands by flowing ozone at RT led to smaller Au particles (1.2 nm) than after calcination at 400 °C (2.7 nm) [55], or the decomposition of dodecanethiol by oxygen plasma treatment at RT led to gold NPs much smaller (3.5 nm) than after thermal treatment at 250 °C in He (10–20 nm) [56], or the removal of PVP by UV-ozone treatment preserved the initial gold particle size (4.9 instead of 4.7 nm) [57].

Recently, other strategies have been tested to remove the SA. Since many of them are water soluble, attempts have been made to remove them by washing, for instance under water reflux at 90 °C in the case of PVA [58,59], and 20% of PVA could be removed and gold particles in $Au/TiO_2$ only slightly increased in size. PVP and some organothiols were removed by washings with solutions containing $NaBH_4$ and/or *tert*-butylamine followed by washing in ethanol/acetone without affecting the size of the NPs [60–62]. Acidic treatments have also been efficient in some cases [63,64].

### *4.1. Colloidal Metal Particles*

Preparations involving the deposition of Au-Pd colloids on activated carbon were widely developed by the Prati's group, using polyvinyl alcohol (PVA) as stabilizer and $NaBH_4$ as reducing agent [65–68]. The best results in terms of single-phase bimetallic particles with small sizes were obtained after sequential reduction-deposition [66], i.e., adsorption of PVA-stabilized gold colloids on activated carbon, followed by palladium reduction on gold nanoparticles by bubbling $H_2$—a reducing

agent milder than $NaBH_4$—in the presence of PVA. As a matter of fact, the second step derives from the redox methods described later in Section 5.3. XRD analyses indicated that the particles were bimetallic. Small Au-Pd nanoparticles of ~3.6 nm were obtained on carbon nanofibers and carbon nanotubes [68]. The method of co-reduction of $HAuCl_4$ and $PdCl_2$ (1:1 molar ratio) by $NaBH_4$ in the presence of PVA has been used by Hutching's group before immobilization on activated carbon at pH 1 after addition of $H_2SO_4$ [69] and on $TiO_2$ [58], and led to particle sizes of 5.1 and 3.8 nm, respectively. Konuspayeva et al. [70] used almost the same type of preparation method to prepare Au-Pd and Au-Rh (a non-miscible system) on $TiO_2$ nanorods, except that adsorption was performed at pH 3.5 using HCl. The authors reported that treatment under $H_2$ or under $O_2$ then $H_2$ at 350 °C was efficient enough to remove PVA without inducing drastic increase in particle size: from 2.5 to around 3 nm in Au-Pd/$TiO_2$ and from 3 to 3.7 nm in Au-Rh/$TiO_2$. Interestingly, electron microscopy revealed that the particles in Au-Pd/$TiO_2$ remained bimetallic after $H_2$ or after $O_2$ then $H_2$ treatment whereas those in Au-Rh/$TiO_2$, turned Janus-type after $H_2$ treatment, and tended to segregate into two separate phases with small Rh particles and larger Au ones after $O_2$ then $H_2$ treatment (Figure 4). PVA was also used to stabilize Au-Ag colloids but first with the synthesis of PVA-stabilized Ag to avoid AgCl precipitation then the addition of $HAuCl_4$ and PVA followed by $NaBH_4$ [71]. Adsorption of the Au-Ag colloids on $TiO_2$ was assisted by poly(diallyldimethylammonium) chloride (PDDA) addition. PDDA acted as a "glue" with its positively charged surface because both the surface charges of the Au-Ag colloids and of the silica support were negatively charged at the applied pH. The samples were washed and dried then calcined in air at 400 °C and reduced in $H_2$ at 350 °C. Based on UV-visible spectroscopy and TEM results, the particles were alloy-type with average size between 2.9 and 5.2 nm depending on the Au/Ag ratio. Based on the same principle, PVA-stabilized Au-Pt colloids with first the synthesis of Pt colloids from $H_2PtCl_6$, PVA and $NaBH_4$ then the reduction of $HAuCl_4$, were adsorbed on multi-walled carbon nanotubes [72]. After treatment in $N_2$ at 350 °C, the particles were ~4 nm and EDX performed on a series of individual NPs showed that most of them were bimetallic.

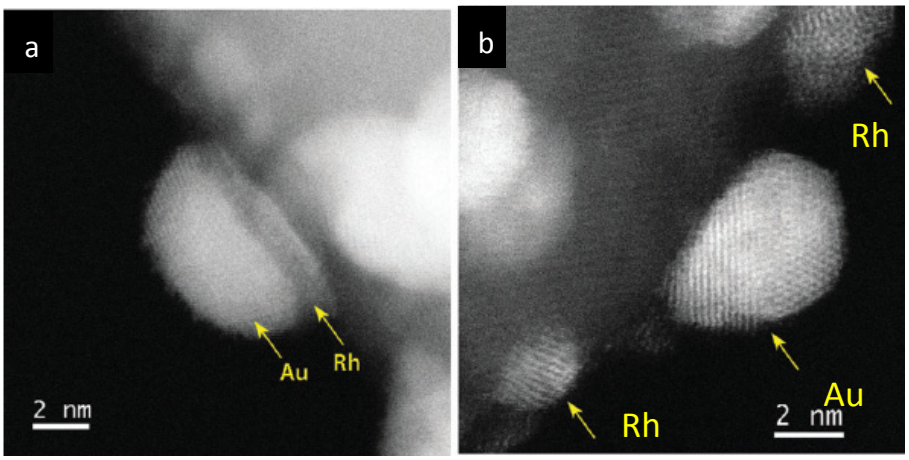


**Figure 4.** Representative aberration-corrected STEM-HAADF images of particles in Au-Rh/$TiO_2$ sample: (**a**) a particle after treatment under $H_2$ at 350 °C showing a segregated "Janus-like" configuration with Au/Rh/$TiO_2$ stacking; (**b**) particles after treatment under $O_2$ then $H_2$ at 350 °C showing metal segregation; smaller ones are Rh and larger ones are Au NPs (more contrasted)—Adapted with permission from [70]. Copyright 2015, Royal Society of Chemistry.

PVP was also used for the preparation of Au-Pd particles by co-reduction of $HAuCl_4$ and $PdCl_2$ with ethanol added to water under reflux under $N_2$ at 90 °C [73]. After adsorption on silica, washing and drying, the particle size was 3.5 nm for the 1:1 Au/Pd ratio but 6.2 nm after calcination at 400 °C and reduction in $H_2$ at 200 °C, and a fraction of the particles were monometallic Pd.

Tetrakis (hydroxypropyl) phosphonium chloride (THPC), which is both a stabilizer and a reducing agent, was used by Baiker et al. [74] to prepare Au-Pd supported on titania, alumina, and silica, after co-reduction of $HAuCl_4$ and $Na_2PdCl_4$ in a basic solution of THPC. After adsorption on the supports at pH 2, washing, drying, and further reduction at 250 °C, the particles were 3.5 nm on alumina, 3.0 nm on $TiO_2$ and 5.6 nm on $SiO_2$. The results of STEM-HAADF, EXAFS and CO-DRIFTS indicated that the particles were bimetallic.

Citrate, which also acts as both a stabilizer and a reducing agent, was used for the preparation of Au-Pd particles on $TiO_2$ [75,76]. Au-Pd/$TiO_2$ was prepared from an aqueous solution of $HAuCl_4$ and $PdCl_2$ reduced by a mixture of sodium citrate and tannin; the average nanoparticle size was 4.2 nm [75]. However, after adsorption on titania at pH 2, and thermal treatment at 400 °C under $O_2$ then at 200 °C under $H_2$, the particles became larger (10 nm). XRD and in situ EXAFS showed that the particles were bimetallic. In ref. [76], the same method was used to prepare Au-Pd/$TiO_2$, but smaller NPs (1 to 5 nm) were obtained after calcination at 350 °C (no red). Au-Pd/graphene was prepared from a graphene oxide in suspension in sodium citrate solution sonicated then heated to 100 °C [77]. A solution of Pd acetate, chloroauric acid, and ascorbic acid was added, and the whole mixture was stirred at 100 °C, inducing also the reduction of graphene oxide into graphene. After washing and drying, the particles were smaller than 10 nm, and STEM-HAADF and EELS revealed the presence of Au core-Pd shell structures (Figure 5). This method was also applied for the preparation of Au-Ag colloids [78]. Note that the $AgNO_3$ precursor solution was diluted enough to avoid AgCl precipitation in the presence of $HAuCl_4$. The colloids were adsorbed on a $TiO_2$ support under UV-irradiation. The resulting sample contained bimetallic particles of around 10 nm-size.

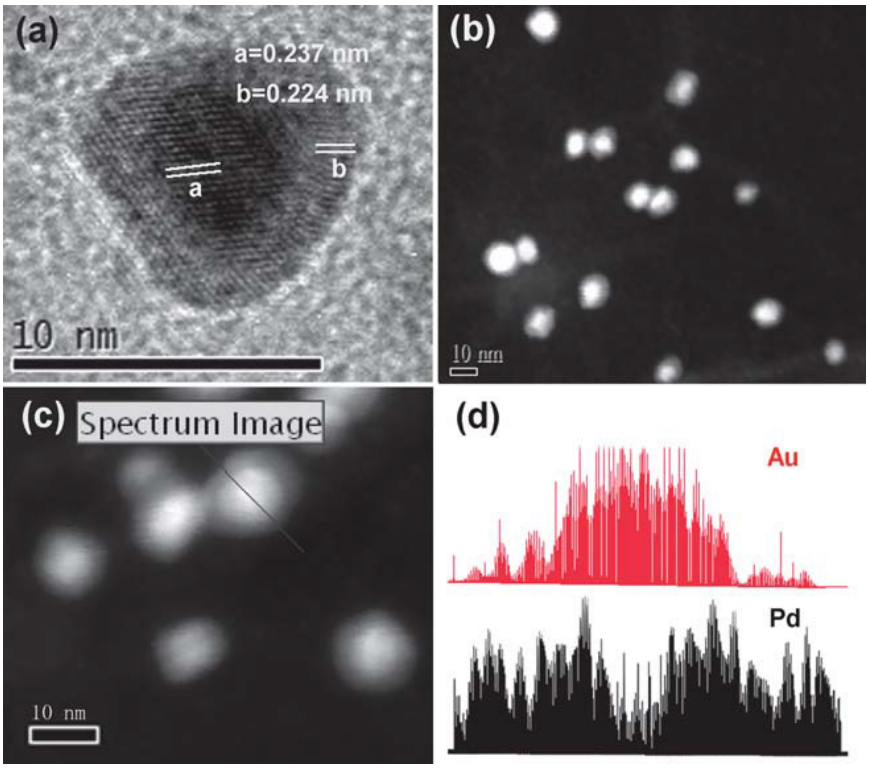


**Figure 5.** HRTEM image (**a**) of a single Au core-Pd shell nanoparticle dispersed on graphene. STEM-HADDF image (**b**) of the hybrids. EELS (electron energy loss spectroscopy) spectrum images (**c**,**d**) of a single nanoparticle—Adapted with permission from [77]. Copyright 2011, Royal Society of Chemistry.

One can find also few examples of colloid preparation in the organic phase. For instance, $TiO_2$-supported Au-Cu nanoparticles with Au:Cu ratios of 3:1, 1:1 and 1:3 were synthesized from

pre-formed thiol-capped nanoparticles in toluene. They were obtained after phase transfer of $AuCl_4^-$ and $Cu^{2+}$ ions from aqueous solution of $HAuCl_4$ and $Cu(NO_3)_2$ to toluene, using tetraoctylammonium bromide as a phase transfer reagent. Dodecanethiol was then added as stabilizer, and reduction proceeded by addition of aqueous solution of $NaBH_4$ [79]. After solvent removal and re-dissolution in toluene, the colloids were impregnated on titania (1.2 wt %). After calcination at 400 °C, the same average particle size (5.6–5.8 nm) was found in all samples, and EELS and HRTEM attested the presence of the same Au–Cu alloy structure.

### *4.2. Metal Particles in Micelles*

Reverse micelles as stabilizers, i.e., water in oil emulsion, are sometimes used to prepare mono and bimetallic particles. Au-M particles (M. Fe, Co, Ni, Cu, Zn) synthesized in reverse micro-emulsion were supported on carbon [80,81]. For instance, in the case of the Au-Ni system, two sets of reverse micelle solutions were prepared by adding AOT (the surfactant, sodium bis(2-ethylhexyl)sulfosuccinate) in n-heptane (the oil phase) separately to an aqueous solution of $HAuCl_4$ and $NiCl_2$ and to one containing $NaBH_4$ [80]. The two sets of reverse micelle solutions were mixed, leading to the formation of metal particles, then the carbon support was added to the solution. After washing and drying then reduction at 250 °C, the particles were uniformly dispersed on carbon with size ~3 nm. The Au/Ni ratios measured by EDX were close to the nominal ones (3:1, 1:1, and 1:3). No direct proof was provided that the NPs were bimetallic but the electrocatalytic results indicated that gold was modified by nickel. The same authors applied this method for the preparation of other Au-M bimetallics on carbon, Au-M/C (M, Fe, Co, Cu, Zn) with a Au:M ratio of 1:1 [81]. The atomic ratios measured by EDX were close to 1:1, and again, the electrocatalytic properties, attested that the particles were bimetallic.

Au-Pd particles on carbon with Au:Pd atomic ratio varying from 0.1 up to 2.1 were also prepared by the reverse "water-in-oil" microemulsion technique [82]. However, in this case, a single aqueous solution of $PdCl_2$ and $HAuCl_4$ was added to the solution of Triton-X-114 (polyoxyethylene(7,8)octylphenyl ether, the surfactant) in cyclohexane (the oil phase), to which hydrazine was then added. The reduction of metal ions was fast, and the color of liquid quickly changed to black. Then, carbon support was introduced, and deposition of metal nanoparticles on the support was carried out by introducing THF (tetrahydrofuran): the liquid became gradually colorless, showing complete deposition of metal particles on the support. After thorough washing with methanol and acetone then with water, the catalysts were dried at 120 °C. The metal particles in the Au-Pd/C catalysts were of 5–8 nm in size. The average particle size of low Au-contents (Au:Pd <0.8) were smaller than Pd (6.7 nm), but the particle size increased with the Au:Pd ratio, and for the one of 2:1, it was only slightly smaller than that of Au (8.2 nm). XRD and EDS analyses indicated Au-Pd alloy formation, and the slight XPS shift in Pd binding energy with respect to that of Pd was also an indication of Au-Pd interaction.

Block copolymer micelles formed by polystyrene-b-poly(4-vinylpyridine) (PS-b-P4VP) in toluene were used as nanoreactors for preparing bimetallic Au-Ag nanoparticles with Au:Ag ratio of 1:1 on several supports, $TiO_2$, nanostructured $TiO_2$ (*n*-$TiO_2$), and $Al_2O_3$ [83]. $AgNO_3$ was first added to PS-b-P4VP in toluene and allowed 24 h for diffusion into the micelle cores, then $HAuCl_4$ was added and left with stirring for 24 h, then the reducer, hydrazine, was added. NPs with an average diameter of 3.1 nm were observed by TEM, and EDX performed on 30 single particles confirmed that all particles contained both Au and Ag with an atomic ratio of 1. The support was mixed with the colloidal solution and the suspension was dried. To remove the polymer shell, a thermal treatment was carried out at 400 °C using pure $H_2$ or $O_2$. After treatment at 400 °C in $H_2$, broader particle size distribution between 5 and 20 nm was obtained on $TiO_2$ whereas on *n*-$TiO_2$, the distribution was much narrower 2 to 7 nm, resulting in an average diameter of 3.1 nm. Using $O_2$ for the thermal treatment, similar small NPs were obtained on *n*-$TiO_2$ while they sintered on $TiO_2$ and alumina (12 nm).

In this last example, interfacially cross-linked reverse micelles (ICRMs) were used to accommodate anionic gold and palladium complexes in their ammonium-lined hydrophilic cores [84]. Unlike

dynamic reverse micelles that constantly exchange surfactants and internal contents with one another, the ICRMs are stable core-shell organic nanoparticles with tunable properties. Deposition onto a solid support ($TiO_2$) followed by thermal treatment led to supported bimetallic nanoparticles. Practically, an aqueous solution of $H_2PdCl_4$ and $HAuCl_4$ was mixed with a solution of ICRM dissolved in chloroform in order to be extracted by the ICRM core. During this step, the complexes were reduced by the bromide counterion in the ICRM core. The organic phase was separated, washed with water, and concentrated in vacuum to give a powder, which was dissolved again in chloroform. This solution was added to $TiO_2$ dispersed in chloroform and stirred. After chloroform evaporation, the sample was heated at 250 °C then at 350 °C under $H_2$ to decompose the ICRMs; metal nanoparticles with average size of 3 nm were obtained. The Pd/Au ratio in the sample was in agreement with the initial loadings. XPS indicated charge transfer from Pd to Au.

### *4.3. Metal Particles in Dendrimers*

The stabilizers of the gold colloids can also be dendrimers, often PAMAM's (polyamidoamines), which are commercially available. These are hyperbranched polymers that ramify from a single core and form a porous sphere [85,86] (Figure 6). Dendrimers are defined by the number of generations and the nature of the termination function, e.g., G4-OH or G6-$NH_2$. Dendrimer-encapsulated nanoparticles (DENs) are synthesized by sequestering metal ions in dendrimers, which are afterwards chemically reduced. One can find several studies exploring the use of DENs to synthesize supported bimetallic catalysts. These DENs can be obtained by co-complexation of both metal salts followed by reduction or through successive complexations then reduction. The experiments must be performed under neutral atmosphere. Several protocols of deposition are proposed: the formation of DENs then support deposition, the use of DENs as nano-reactors to form bimetallic particles that are then extracted and deposited on a substrate, and the use of DENs to template the porosity of the support (Section 6.1).

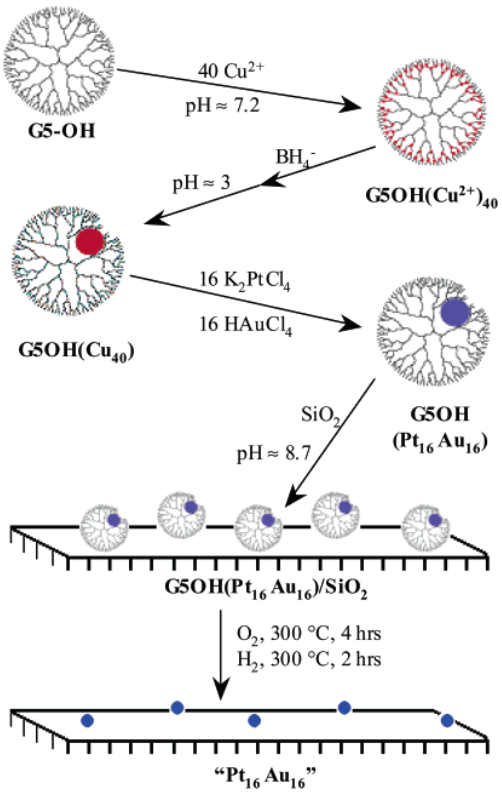


**Figure 6.** Preparation process of Au-Pt NPs on silica support involving the synthesis of Au-Pt NPs in dendrimers. Copied with permission from [87]. Copyright 2004, American Chemical Society.

Initially, the synthesis of bimetallic particles in dendrimers was developed to overcome the difficulty of preparing bimetallic particles with a miscibility gap, such as Au-Pt, Au-Ni or Au-Ir. For example, hydroxy-terminated fifth generation PAMAM dendrimers (G5-OH) were used to synthesize Au-Pt DENs before deposition on silica, alumina, and titania [87,88]. However, because of the large standard potential of the aurate ion (+1 V vs. NHE), the Au and Pt precursors could not be directly reduced in dendrimers. Therefore, a "Cu exchange" method was proposed, involving G5-OH PAMAM dendrimers in preparing Cu nanoparticles; the latter then acted as in situ reducing agent for $HAuCl_4$ and $K_2PtCl_4$ (1:1) (Figure 6); this is in fact a galvanic replacement reaction as developed later in Section 5.3. After adsorption of the Au-Pt DENs onto the different supports cited above, the samples were washed with EDTA solution to remove the remaining Cu, then calcined and reduced under $H_2$ at 300 °C. TEM, EDS, and CO-FTIR spectroscopy showed that this preparation route resulted in nanoparticles in which the two metals were intimately mixed, and that most of the bimetallic nanoparticles were smaller than 3 nm. For the preparation of Au-Ni/$TiO_2$, the method applied was more complex [89]. Ammine-terminated G5 PAMAM dendrimers were first grafted to a silica support via a siloxane-linked anhydride. The dendrimers were then alkylated and used to template the Au-Ni nanoparticles resulting from the co-reduction of $NiCl_2$ and $HAuCl_4$ with $NaBH_4$. These nanoparticles were subsequently extracted from the supported dendrimers by toluene containing decanethiol that acted as new capping ligand. The thiol-stabilized Au-Ni particles were separated by centrifugation. After adsorption on $TiO_2$, the thiol ligands were decomposed under $H_2$ at 300 °C. TEM, EDS, and CO-DRIFTS indicated the presence of bimetallic nanoparticles of ~3 nm with a Ni core-Au shell structure. In this other example, four sequential synthesis routes involving G4-OH PAMAM dendrimers were tested to produce bimetallic Au-Ir particles (Figure 7), which were afterwards supported on alumina [90]. The sample containing *in fine* the smallest metal particles (1.6 nm) was the one prepared from $IrCl_3$ solution mixed first with the dendrimer solution for 7 days under $N_2$ to allow complexation without $Ir^{3+}$ oxidation. Then, $HAuCl_4$ solution was added, and complexation readily took place. The resulting solution was used for alumina impregnation, followed by calcination at 350 °C then reduction at 400 °C.

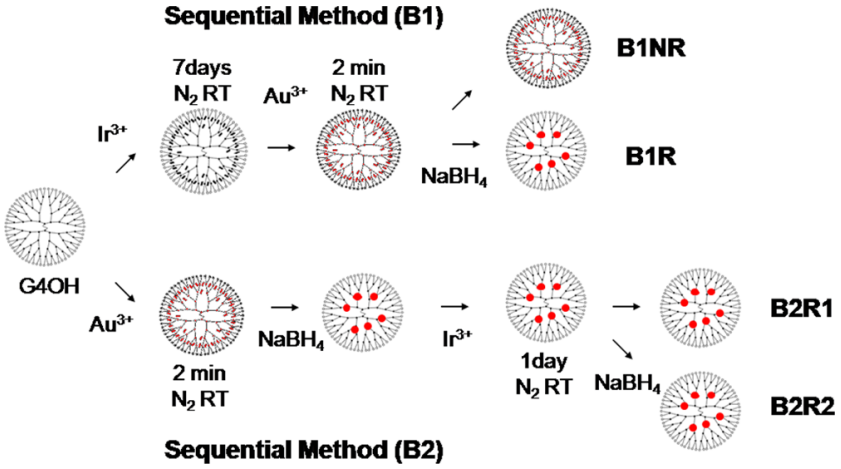


**Figure 7.** Four sequential method of preparation of bimetallic Au-Ir particles in dendrimers before impregnation on alumina: (B1) $IrCl_3$ then $HAuCl_4$ adsorption (B1NR) and reduction with $NaBH_4$ (B1R); (B2) $HAuCl_4$ adsorption and reduction with $NaBH_4$ then $IrCl_3$ adsorption (B2R1) and reduction with $NaBH_4$ (B2R2). Copied with permission from [90]. Copyright 2013, American Chemical Society.

For "easier" bimetallic systems, such as Au-Pd, the nanoparticles can be synthesized in dendrimers by complexation of $K_2PdCl_4$ then of $HAuCl_4$, followed by chemical reduction with $NaBH_4$. This was done for the synthesis of Au-Pd (1:1) in G4-PAMAM built in the channels of SBA-15 [91] (see Section 6.2).

### *4.4. Microwave-Assisted Reduction*

Several protocols of microwave-assisted reduction can be applied to the preparation of bimetallic catalysts: co-reduction before deposition onto a support, co-reduction in the presence of a support and sequential reduction-deposition. One can note that the temperatures reached during microwaving are scarcely reported.

In this example, bimetallic Au-Cu particles were prepared with microwave assistance before deposition on a $TiO_2$ support. The Au-Cu colloids (1:1) were synthesized by co-reduction of $HAuCl_4$ and $CuSO_4$ by glucose in an alkaline aqueous solution containing PVP [92]. Microwaving allowed the solution to rapidly reach the temperature of 90 °C, and to induce rapid reduction of the metal precursors. The Au-Cu colloids were then immobilized onto $TiO_2$ by solvent evaporation and drying. EDS of individual particles (4.4 nm in average) showed that the particles were bimetallic. No ordering or segregation effects were observed by STEM-HAADF and the Au:Cu ratio was quite constant irrespective of the particle size.

Au-Pt nanoparticles supported on carbon black (10 wt % Pt + 10 wt % Au) were prepared by microwave-assisted polyol reduction method, i.e., by co-reduction of $HAuCl_4$ and $H_2PtCl_6$ in the presence of the support in suspension in ethylene glycol [93]. After pH adjustment to 10, the suspension was microwaved under stirring. After washing and drying, the average metal particle size was 3.3 nm and after thermal treatment at 500 °C under $H_2$, it was 4.7 nm. XRD showed that the position of the diffraction peaks of the metal particles were between those of Au and Pt NPs, indicating the formation of Au-Pt nanoalloy. Au and Pt being immiscible, the alloy formation was attributed to the fast reduction rates of both metal ions under microwave conditions. However, the thermal treatment enabled the migration of Au atoms from the subsurface to the particle surface, as attested by XPS.

The last example concerns the preparation of Au-Ag nanoparticles into porous carbon spheres. First, Ag nanoparticles were synthesized by microwaving an aqueous suspension of carbon in which $[Ag(NH_3)_2]^+$ was pre-adsorbed and to which PVP was added [94]. Metal Ag nanoparticles with a diameter of ~10 nm were formed in the porosity of the carbon spheres. During microwaving, the Ag ions were reduced by electrons arising from the carbon support. Au was then incorporated by immersion of Ag/C in a $HAuCl_4$ solution at RT without additional reducing agent. The particles were larger than 10 nm, and STEM-EDS revealed particles with Ag core-Au shell structure. The same procedure was used by the same authors for the preparation of Au-Pd nanoparticles into porous carbon spheres [95]; $Ag(NH_3)_2(NO_3)$ was replaced by $PdCl_2$.

## 5. Specific Methods for the Preparation of Bimetallic Catalysts

### *5.1. Bimetallic Clusters*

Organo bi-metallic precursors are sometimes used for the preparation of supported bimetallic particles. Once they are supported, the samples are thermally treated in order to decompose the precursors and form the bimetallic NPs. One can find only very few examples concerning gold-based bimetallics. $Pt_2Au_4(C{\equiv}CtBu)_8$ was adsorbed onto silica from hexane solution; after calcination at 300 °C and reduction at 200 °C, this led to ~2.5 nm particles of alloy-type according to the TPR and CO-DRIFTS characterization results [96]. $[NEt_4][AuFe_4(CO)_{16}]$ is another precursor, which was impregnated on titania, but after decomposition at 400 °C in $N_2$, gold nanoparticles (from 3 to 7 nm for Au loadings from 2 to 7 wt %) were found anchored onto the titania surface through an iron oxide interface [97].

### *5.2. Radiolysis-Assisted Reduction*

Radiolytic reduction of metal ions in aqueous solutions is a method suitable for the synthesis of mono and bimetallic nanoparticles, but in the case of supported materials, this method has been used only for the synthesis of bimetallic NPs. The principle is the following: the hydrated electrons and the reducing radicals produced during the radiolysis of water by irradiation with $\gamma$-rays or accelerated

electrons, reduce the metal ions. Depending on the dose rate, alloy-type or core-shell particles can be formed. Reduction can be performed either before support adsorption, which requires the addition of stabilizing agent, or directly in the presence of the support.

Au-Pd nanoparticles were produced by radiolysis, then adsorbed on an alumina support [98]. The aqueous solution containing $HAuCl_4$ and $Pd(NO_3)_2$ was irradiated under a $N_2$ atmosphere in the presence of PVA as stabilizing agent and of 2-propanol as scavenger of oxidizing OH• radicals. Under $\gamma$ irradiation, Au core-Pd shell particles of 3–4 nm were obtained whereas under electron beam, i.e., at higher dose rate, very fast reduction occurred and alloy-type nanoparticles of 2–3 nm were formed. After adsorption on alumina, washing and drying, reduction at 300 °C was performed to remove PVA. This led to particle reconstruction in both cases without drastic change of size (~3 nm) but with different proportions of Pd on the particle surface.

Radiolysis can also be used to overcome the difficulty of preparing bimetallic nanoparticles with a miscibility gap. Bimetallic Au-Pt nanoparticles (1:0.75) were prepared by reduction of $H_2PtCl_6$ and $HAuCl_4$ under $\gamma$-rays in an aqueous solution containing PVA and polyacrylic acid (PAA) [99]. After adsorption onto a silica support, calcination at 400 °C then reduction at 500 °C, the metal particles were 4.6 nm in size. The characterization by XRD, TEM-EDS, and CO-FTIR indicated that the particles, which had a Au core-Pt shell structure after radiolysis, transformed into an alloy-type structure with a Au-rich surface after deposition on silica and thermal treatments.

Radiolysis can also be performed directly in the presence of the support and without stabilizer. An aqueous solution containing $HAuCl_4$ and $H_2PtCl_6$ (1:1), 2-propanol and $\gamma$-$Fe_2O_3$ powder in suspension was irradiated by electron beam [100]. The resulting particles were 2.9 nm, and the XRD peak located between those of Pt(111) and Au(111) indicated that the particles were bimetallic.

### *5.3. Surface Redox Methods*

Methods based on surface reduction-oxidation (redox) reactions to prepare supported bimetallic catalysts were developed first by Barbier and colleagues [101–103], then more recently by Monnier and colleagues [104,105]. They are based on the principle that a second metal can be deposited on the first one already supported, thanks to a redox reaction selectively occurring on the particle surface of the first metal.

This can be achieved by the so-called "direct surface redox reactions", or also called "galvanic replacement reaction (GRR)", i.e., by a redox reaction between the oxidized precursor of the second metal in aqueous solution and the pre-reduced supported particles of the first metal (Figure 8a). This occurs spontaneously when the redox potential of the second metal is higher than that of the first metal. Hence, the precursor of the second metal is reduced on the first metal, and the latter is oxidized and dissolved in the solution, and therefore also acts as a sacrificial component.

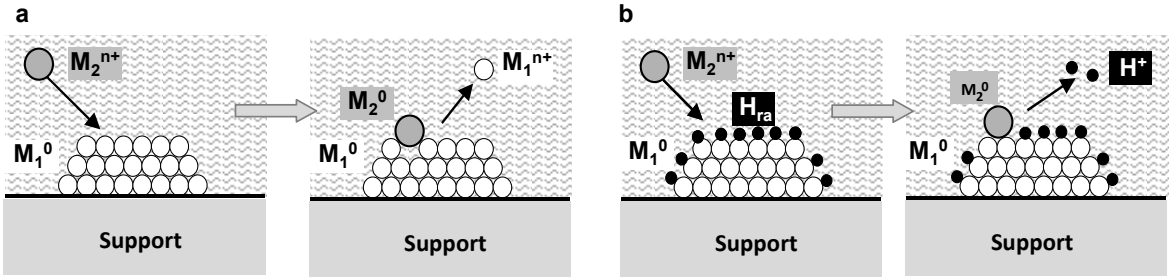


**Figure 8.** Schematic illustration of the surface redox methods: (**a**) Direct reduction of $M_2^{n+}$ ions by $M_1^0$ metal particle, also called galvanic replacement reaction; (**b**) Reduction of $M_2^{n+}$ ion by active H adsorbed on $M_1^0$ metal particle resulting from $H_2$ dissociation or activation of a reducing agent on $M_1^0$.

Surface redox preparation can also be achieved through a "redox reaction assisted by a reducing agent" adsorbed or activated on the pre-reduced catalyst, for instance hydrogen dissociatively adsorbed

on the first metal (Figure 8b) [101–103] or a reducing agent such as dimethylamine borane or hydrazine, activated by the first supported metal [104,105]; this method is also called "Electroless Deposition" (ED). Note that successful redox deposition requires that the reducing agent cannot reduce the precursor of the second metal in solution (or that its kinetic of reduction is much longer than that of reduction on the first metal), and that the precursor cannot adsorb onto the support. All these methods have been applied to the preparation of gold-based bimetallic catalysts. In principle, these methods do not require further thermal treatments since both metals are supposed to be reduced during the preparation, but they may re-oxidize in air during transfer in the catalytic reactor. Therefore, a mild reduction treatment at around 200 °C is often applied before reactions.

Au-Ag bimetallic NPs were synthesized by GRR on microspheres containing a $Fe_3O_4$ core and a carbon shell [106]. The addition of a solution of $HAuCl_4$ to metallic Ag nanoparticles supported on these microspheres, followed by incubation at 50 °C, led to the formation of the Ag-Au particles. Indeed, the standard reduction potential of the $AuCl_4^-$/Au pair (0.99 V vs. SHE (standard hydrogen electrode)) is higher than that of the $Ag^+$/Ag pair (0.80 V vs. SHE), so the Ag particles are oxidized into $Ag^+$ ions, which are leached out, and $HAuCl_4$ is reduced on the Ag particles. Bimetallic Au-Ag NPs supported on $TiO_2$ were also obtained through GRR, between photo-deposited Ag/$TiO_2$ and aqueous $HAuCl_4$ solution heated under reflux [107]. The particle size remained almost unchanged (1.5 nm). Au-Cu/$TiO_2$ was synthesized by a one-pot photodeposition-GRR method [108]: After deoxygenation and pH adjustment to 7, the suspension of $TiO_2$ in a solution of Cu acetate in water and ethanol was UV-irradiated to photo-deposit Cu nanoparticles onto $TiO_2$. Then, a deoxygenated $HAuCl_4$ solution was added to perform GRR in the dark. Small-size metal nanoparticles (<2 nm) with Au-rich core/Cu shell structure were found dispersed on the $TiO_2$ surface.

The redox method with pre-adsorbed hydrogen was applied to the preparation of Au-Pd/$SiO_2$ catalysts: A de-aerated solution of $HAuCl_4$ was added to an aqueous suspension of reduced Pd/$SiO_2$ on which hydrogen was pre-adsorbed by bubbling $H_2$ [109]. After washing and drying, the sample was calcined at 300 °C and reduced at 200 °C. The initial Pd particle size was 3.5 nm, and 4.3 nm after gold deposition and thermal treatment, and the particles were alloy-type. The same procedure was used for a titania support [110]. EDS showed the presence of both Au and Pd in the particles with a composition close to the metal loadings, but no particle size was reported in the paper. The redox method with pre-adsorbed hydrogen was also used to prepare bimetallic nanoparticles from non-miscible metals. Bimetallic Au-Pt/$SiO_2$ catalysts were prepared by depositing Au (up to 2.2 wt %) from a $HAuCl_4$ solution at pH 1 on Pt/$SiO_2$ (6.3 wt %) containing Pt particles of 2.7 nm [111]. After washing and drying, the particles were bimetallic according to EDS measurements, but they were much larger than initially (6.5 nm) because of sintering in the liquid phase. Au-Ru/C samples were also prepared according to the same principle [112]. In this case, after gold deposition (0.85 wt %) on a Ru/C catalyst (5 wt %), the particles were slightly larger (2.9 nm) than the Ru particles (2.6 nm). However, their composition was at variance. EDS measurements revealed that those in the 1.5–3 nm range contained mainly Ru, while those in the mid-size range (5–10 nm) contained both Au and Ru, and the few larger ones (>10 nm) mainly contained Au.

Up to now, electroless deposition (ED) with gold has been applied only to the preparation of Au-Pd particles supported on silica [113,114] and on carbon [115]. Au ED was performed at pH 9 on large Pd particles of commercial Pd/$SiO_2$ catalysts, using $KAu^{I}(CN)_2$ as precursor and hydrazine as the reducing agent, which was activated onto the Pd particles. Note that under such experimental conditions, gold reduction occurs only on Pd particles and not in solution and the pH conditions prevented electrostatic interaction of the gold precursor with the support. After ED completion (around 2 h) and thorough washing, EDS, CO-DRIFTS, and XPS characterization showed that the particles were bimetallic; the results also showed that the coverage of Pd by Au could be controlled by the amount of gold in the ED solution. For the preparation of Au-Pd/C [115], the same protocol was adopted with Pd/C, except that the solution was heated at 40 °C and pH was adjusted to 12.

## 6. Gold-Based Bimetallic NPs Embedded in a Matrix

In this section, several strategies of synthesis of gold-based bimetallic nanoparticles embedded into inorganic matrices containing opened porosity are presented. They involve the addition of metal precursors or preformed metal particles during the synthesis of the matrices prepared either by precipitation or sol-gel, or post-synthesis through their addition in the porosity. A sub-section is also devoted to the synthesis of NPs in an inorganic-organic matrix of the MOF-type.

### *6.1. Embedding during Synthesis of Inorganic Matrix*

One method is the co-precipitation, which allows a one-pot preparation of both the bimetallic particles and the oxide supports, such as $\alpha$-$Fe_2O_3$, $Co_3O_4$, $MnO_2$, CuO, $CeO_2$, and ZnO. Co-precipitation is generally performed by addition of sodium carbonate to aqueous solutions containing $HAuCl_4$, the second metal precursor and the nitrate precursor of the oxide support at controlled pH and temperature. After aging, the co-precipitate is washed thoroughly to remove sodium and chlorides, dried, and thermally treated to form metallic particles and to transform the oxy-hydroxy-carbonate precipitate into oxide. In fact, co-precipitation is barely used for the preparation of bimetallic particles in matrices. However, one can cite one example with the preparation of Au-Pt/$CeO_2$ from an aqueous solution containing $H_2PtCl_6$ and $HAuCl_4$, $Ce(NO_3)_3$, and urea, which was aged at 100 °C for 50 h [116]. After calcination at 500 °C, the metal particles were 5–10 nm and bimetallic, and they were larger than Au and Pt in monometallic samples, 5–6 and 2–3 nm, respectively.

Metal precursors or bimetallic colloids are rather introduced in sol-gel precursor mixtures of the oxide matrices. One can first cite the case of the synthesis of Au-Cu particles in $SiO_2$, $ZrO_2$, and $TiO_2$ performed by introduction of $HAuCl_4$ and $CuCl_2$ salts into the sol precursors containing alkoxides [117]. After drying, calcination and reduction at 500 °C, the particles were bimetallic and of alloy-type with sizes between 25 and 38 nm depending on the nature of the matrix.

Bimetallic colloids can be mixed with sol-gel mixtures, for instance for embedding of Au-Pd colloids in mesoporous silica [118]. Tetraalkylammonium-stabilized Au-Pd colloids dispersed in THF were added to a sol-gel mixture of TEOS, THF, $H_2O$, and HCl. No increase in the bimetallic particle size, initially of 3 nm, was observed after the mesoporous silica has been formed and even after thermal treatments under $O_2$ and then under $H_2$ at 450 °C, carried out to eliminate the organics. PVP-stabilized Au-Pd colloids with several Au/Pd ratios, and synthesized either by co-reduction of the precursors in methanol by $NaBH_4$ or by sequential reduction of $K_2PdCl_4$ in methanol by $NaBH_4$ then of $HAuCl_4$ by ascorbic acid, were added to a alumina-precursor sol-gel mixture [119]. After calcination and reduction at 300 °C to form alumina and remove PVP, the metal particles arising from co-reduction had a slightly Au-rich core and Pd-rich shell, and were slightly larger (5.5 nm) than in colloids (4.1 nm). In contrast, those arising from sequential reduction maintained their initial Pd core-Au shell structure and size (5.5 instead of 5.2 nm).

Au-Ni nanoparticles of 3–4 nm synthesized in reversed-micelles (Section 4.2) were embedded in 15 nm silica nanospheres. The NPs arose from $Au(en)_2Cl_3$ and $Ni(NH_3)_6Cl_2$ introduced in a cyclohexane solution of polyethylene glycol mono-4 nonylphenyl ether (NP-5), which were reduced with $NaBH_4/NH_3BH_3$ [120]. Ammonia solution then tetraethoxysilane (TEOS) was added to the micelles for the sol-gel synthesis.

We found only one example of synthesis involving the use of dendrimers. They were used to template the porosity of a support during sol-gel synthesis and to encapsulate bimetallic nanoparticles (Section 4.3). Au-Pd/$TiO_2$ was prepared from G4-PAMAM dendrimers in which Au-Pd NPs were synthesized [121], then the DENs were added to a solution of titanium isopropoxide in methanol, which was gradually hydrolyzed with $H_2O$. After aging, washing and drying, the average particle size was 1.8 nm, but increased to 3.2 nm after thermal treatments of calcination and reduction in $H_2$ at 500 °C to decompose and eliminate the dendrimers. EDS indicated homogeneous composition from one particle to another, close to 1:1.

### *6.2. Embedding after Matrix Synthesis*

This mainly concerns mesoporous matrices with controlled and structured porosity.

Bimetallic Au-Pd nanoparticles of 1.5 nm size were synthesized in G4-PAMAM dendrimers built into the channels of SBA-15 [91]. G4-PAMAM-SBA-15 powder was dispersed in HCl aqueous solution of pH 2. Then, aqueous solutions of $K_2PdCl_4$ and $HAuCl_4$ were added dropwise. After stirring, the solid was washed and dried at 50 C. The metal was reduced in an excess of $NaBH_4$. After filtration and drying, the bimetallic NPs were well-distributed inside the channels, with an average size of about 1.5 nm. HRTEM and EDS analysis of two particles attested that Pd/Au alloy NPs were obtained.

Highly ordered silica material SBA-16 with cage-like mesopores was synthesized and used to confine the formation of Au-Pd bimetallic nanoparticles [122]. Surface functionalized SBA-16 with APTES (3-aminopropyl triethoxysilane) was positively charged due to the hydrolysis of $–NH_2$ groups, which allowed easy adsorption of negatively charged $PdCl_2(OH)_2^{2-}$ and $AuCl_4^-$ at 80 °C for 5 h. The samples were washed then dried before reduction in $H_2$ at 400 °C. The mean Au-Pd NPs diameters (Au/Pd = 1/3 and 1/6) were around 6 nm, which coincided with the inner diameter of the SBA-16 super-cage. Combined EDX, UV-visible, XRD, and HRTEM allowed to propose that the particles consist of islands of Pd clusters on the surface of a larger Au-rich core. Such a structure was explained by the fact that $Au^{3+}$ has a higher redox potential (1.498 V) than that of $Pd^{2+}$ (0.951 V), therefore the reduction of $Au^{3+}$ is faster, and metallic Pd is expected to form afterwards.

The method of successive reduction developed by Liu et al. for the preparation of Au-Cu and Au-Ag in $SiO_2$ and SBA-15 has been already described in Section 3.1 and Figure 2. The support was first functionalized with APTES, and this was followed by $HAuCl_4$ adsorption-$NaBH_4$ reduction then after washing and drying by $Cu(NO_3)_2$ adsorption-$NaBH_4$ reduction [41,43] or $Ag(NO_3)_2$ deposition-$NaBH_4$ reduction [42]. Again, after washing and drying, the solid was calcined at 500 °C to remove APTES then reduced at 550 °C in $H_2$, leading to small bimetallic particles in the porosity. This method was reused by several authors for the preparation of Au-Ag in mesoporous materials [123–126].

### *6.3. Embedding in Inorganic-Organic Matrix*

This section concerns Metal Organic Frameworks (MOFs), also called Porous Coordination Polymers (PCPs), which are 3-D structures of an organometallic polymer containing metal cations centers linked by organic ligands. One can find a few examples of synthesis of gold-based bimetallic NPs in MOFs. In all cases, the bimetallic particles were prepared post-MOF synthesis. The challenge is to synthesize the particles in the porosity of the 3-D structures.

The first example of synthesis of gold-based bimetallic particles in MOF was published in 2011 [127]. Au-Ag core-shell NPs were immobilized on a MOF ZIF-8, which is a 3D structure consisting of a $Zn(MeIM)_2$ framework where MeIM = 2-methylimidazole. Two sequential deposition-reduction protocols were used, Au then Ag and Ag then Au. ZIF-8 previously activated under vacuum at 300 °C was suspended in methanol to which a methanol solution of $HAuCl_4$ or $AgNO_3$ was added before further addition of $NaBH_4$ in methanol. After washing and drying at RT, the sample was used for the deposition-reduction of the second metal according to the same protocol as for the first step. In both cases, core-shell particles formed, according to STEM-HAADF and EDS; XPS revealed Au-rich core and Ag-rich shell for both types of samples with similar particles sizes from 2 to 6 nm and the presence of few aggregates (Figure 9). In the case of Ag then Au deposition-reduction, galvanic replacement occurred (Section 5.3) so when $NaBH_4$ was added in the second step, dissolved $Ag^+$ and remnant $Au^{3+}$ were co-reduced, leading to Au core-AuAg shell NPs. The results also revealed that the porous surface structure of ZIF-8 offered steric restriction to confine and prevent the growth of Au/Ag NPs although the particles were larger than the pore sizes of ZIF-8 (1.16 nm).

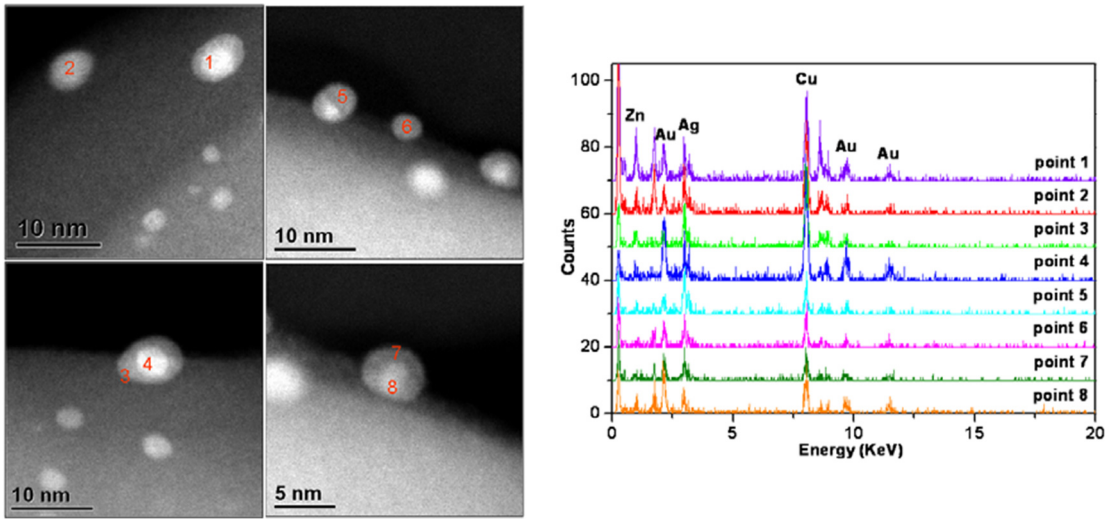


**Figure 9.** HAADF-STEM images (**a**) and the corresponding EDS spectra (**b**) for as-synthesized 2%Ag–2%Au/ZIF-8 sample. The copper signal originates from Cu grid—Adapted with permission from [127]. Copyright 2011, American Chemical Society.

A second paper was published the same year on the preparation of bimetallic Au-Pd nanoparticles in MOF MIL-101. This is also a 3-D structure forming mesoporous cages built with trimers of Cr(III) oxide octahedra and dicarboxylate linkers but containing much larger pore sizes (2.9–3.4 nm) and window sizes (1.2–1.4 nm) than ZIF-8. Au and Pd were introduced in MIL-101 and ethylenediamine (ED)-grafted MIL-101 (ED-MIL-101) by co-impregnation with an aqueous solution containing $HAuCl_4$ and $H_2PdCl_4$ [18]. With ED-MIL-101, electrostatic interaction occurred between the cationic $NH_4^+$ group of ED and the anionic metal species ($AuCl_4^-$ and $PdCl_4^{2-}$) in acidic condition. After reduction at 200 °C, Au-Pd bimetallic particles were obtained but with smaller size in ED-MIL-101 (2–8 nm range with 20 wt % Au + Pd) than in MIL-101 (2–15 nm range). However, only the 2–3 nm size particles could be located inside the mesoporous pores, while the remaining NPs were immobilized on the surfaces of MIL-101 and ED-MIL-101.

PVP-colloids of Au-Pd obtained by co-reduction of $HAuCl_4$ and $PdCl_2$ by $NaBH_4$ in the presence of PVP at 0 °C were adsorbed in MIL-101 [128]. After washing and drying, the sample was heated in $H_2$ at 200 °C, leading to NPs of 2.4 nm in average, but their location was not investigated.

To circumvent the problem of formation of particles outside the MOF pores, another synthesis strategy was elaborated. Xu et al. developed a preparation method combining the so-called "double-solvent" method of preparation and the so-called "overwhelming reduction" (OWR) approach to successfully form and encapsulate Au-Ni [129], Au-Co [130] nanoparticles into the pores of MIL-101. The double-solvent method prevents the diffusion of the precursor compounds and products out of the pores of the host and the formation of NPs on the external surface of MOFs. The procedure was the following: MIL-101 previously activated under vacuum at 160 °C was suspended in dry *n*-hexane, the hydrophobic solvent. Then, an aqueous solution, the hydrophilic solvent, with a volume smaller than the MOF pore volume and containing $HAuCl_4$ and $NiCl_2$ [129] or $HAuCl_4$ and $CoCl_2$ [130] was added dropwise. It entered into the pores because of the hydrophilic character of the Cr-cluster trimer building block. After filtration and drying under vacuum, reduction was carried out with $NaBH_4$ with a pore-volume of solution that can also be incorporated into the pores by capillary force, and with a concentration high enough (0.6 M) to rapidly reduce all the metal precursors deposited in the pores of the MOF. This resulted in the formation of highly dispersed Au-Ni or Au-Co alloy NPs with average size of 1.8 nm encapsulated within the pores of MIL-101 and without deposition of the NPs on the external surface, as attested by various techniques of electron microscopy, HAADF-STEM, EDX and

electron tomographic reconstruction. This method was further used by another group to prepare Au-Pd particles (2.8 nm) in MIL-101 from $HAuCl_4$ and $PdCl_2$ [131].

## 7. Conclusions

As the basis of the conclusion, which also applies to other types of bimetallic systems, several remarks can be made:

The preparation methods based on deposition-reduction allow to generate bimetallic particles after thermal reduction; a fundamental question that would deserve deeper investigations is whether the bimetallic character of the particles builds during the reduction step or whether there is a driving force during precursor deposition (co- or successive deposition), which would favor interaction between the two precursors onto the support and afterwards the formation of bimetallic particles.

The preparation methods involving reduction-deposition, with the deposition of preformed bimetallic particles, take advantage of previous knowledge gained in the field of colloid chemistry on the mechanism of formation of bimetallic particles. Hence, the conditions of formation of some bimetallic systems are already well-known. The main issue with reduction-deposition is the possible evolution of the structure, composition, and size of the particles once they are deposited on a support, and especially when they are submitted to the thermal treatments performed to eliminate the stabilizing agents. The important issue of the reduction-deposition procedure is therefore to develop alternative methods to eliminate the stabilizing agents at lower temperature in order to minimize these changes.

The preparation methods based on surface redox reactions are also very attractive. These methods have been used for a long time for metal plating. However, it is only recently that they have been applied to catalyst preparation, after the first studies published by Barbier and colleagues in the 90 s. However the use of these methods is not straightforward as it requires careful preliminaries to find the right experimental conditions to avoid deposition of the ions of the second metal onto the support or their reduction in solution or in the case of galvanic replacement, the redeposition of the first metal onto the support after it has been re-oxidized by the second one (Figure 8).

Regarding the *embedding methods*, the main issue is the complete removal of the surfactant and/or stabilizing agents in conditions as soft as possible to avoid metal particle growth and structure changes especially when pre-formed metal particles are used, all the more because the thermal treatment requires most often both a calcination and a reduction.

It is noticeable that for the samples prepared according to all these methods, the residual contents of the elements entering into the composition of the metal precursors, precipitating agents, reducing agents etc. are barely reported although they may have a non negligible effect on the catalytic properties.

These remarks, which are certainly not exhaustive, show that there are still many things to learn, to understand, and to do in the field of the preparation of bimetallic catalysts, independently to the fact that the bimetallic particles may restructure during catalytic reactions.

**Conflicts of Interest:** The author declares no conflict of interest.

## References

1. Haruta, M.; Kobayashi, T.; Sano, H.; Yamada, N. Novel gold catalysts for the oxidation of carbon monoxide at a temperature far below 0 °C. *Chem. Lett.* **1987**, *2*, 405–408. [CrossRef]
2. Haruta, M.; Saika, K.; Kobayashi, T.; Tsubota, S.; Nakahara, Y. Preparation and catalytic properties of gold finely dispersed on beryllium oxide. *Chem. Exp.* **1988**, *3*, 159–162.
3. Haruta, M. Size- and support-dependency in the catalysis of gold. *Catal. Today* **1997**, *36*, 153–166. [CrossRef]
4. Wolf, A.; Schüth, F. A systematic study of the synthesis conditions for the preparation of highly active gold catalysts. *Appl. Catal. A Gen.* **2002**, *226*, 1–13. [CrossRef]
5. Louis, C. Gold nanoparticles: Recent advances in CO oxidation. In *Nanoparticles and Catalysis*; Astruc, D., Ed.; Wiley-VCH: Weinheim, Germany, 2008.

6. Widmann, D.; Behm, R.J. Activation of molecular oxygen and the nature of the active oxygen species for CO oxidation on oxide supported Au catalysts. *Acc. Chem. Res.* **2014**, *47*, 740–749. [CrossRef] [PubMed]
7. Liu, J.-H.; Wang, A.-Q.; Chi, Y.-S.; Lin, H.-P.; Mou, C.-Y. Synergistic effect in an Au-Ag alloy nanocatalyst: CO oxidation. *J. Phys. Chem. B* **2005**, *109*, 40–43. [CrossRef] [PubMed]
8. Sandoval, A.; Aguilar, A.; Louis, C.; Traverse, A.; Zanella, R. Bimetallic Au-Ag/$TiO_2$ catalyst prepared by deposition-precipitation. High activity and stability in CO oxidation. *J. Catal.* **2011**, *281*, 40–49. [CrossRef]
9. Iizuka, Y.; Inoue, R.; Miura, T.; Morita, N.; Toshima, N.; Honma, T.; Oji, H. Chemical environment of Ag atoms contained in Au Ag bimetalliccatalysts and the generation of the catalytic activity for CO oxidation. *Appl. Catal. A Gen.* **2014**, *483*, 63–75. [CrossRef]
10. McEwan, L.; Julius, M.; Roberts, S.; Fletcher, J.C.Q. A review of the use of gold catalysts in selective hydrogenation reactions. *Gold Bull.* **2010**, *43*, 298–306.
11. Cárdenas-Lizana, F.; Keane, M.A. The development of gold catalysts for use in hydrogenation reactions. *J. Mater. Sci.* **2013**, *48*, 543–564. [CrossRef]
12. Mitsudome, T.; Kaneda, K. Gold nanoparticle catalysts for selective hydrogenations. *Green Chem.* **2013**, *15*, 2636–2654. [CrossRef]
13. Edwards, J.K.; Solsona, B.E.; Landon, P.; Carley, A.F.; Herzing, A.; Kiely, C.J.; Hutchings, G.J. Direct synthesis of hydrogen peroxide from $H_2$ and $O_2$ using $TiO_2$-supported Au-Pd catalysts. *J. Catal.* **2005**, *236*, 69–79. [CrossRef]
14. Sankar, M.; He, Q.; Morad, M.; Pritchard, J.; Freakley, S.J.; Edwards, J.K.; Taylor, S.H.; Morgan, D.J.; Carley, A.F.; Knight, D.W.; et al. Synthesis of stable ligand-free gold palladium nanoparticles using a simple excess anion method. *ACS Nano* **2012**, *6*, 6600–6613. [CrossRef] [PubMed]
15. Hugon, A.; Delannoy, L.; Krafft, J.-M.; Louis, C. Supported gold-palladium catalysts for selective hydrogenation of 1,3 butadiene in an excess of propene. *J. Phys. Chem. C* **2010**, *114*, 10823–10835. [CrossRef]
16. Yang, X.; Huang, C.; Fu, Z.; Song, H.; Liao, S.; Sud, Y.; Du, L.; Li, X. An effective Pd-promoted gold catalyst supported on mesoporous silica particles for the oxidation of benzyl alcohol. *Appl. Catal. B Environ.* **2013**, *140–141*, 419–425. [CrossRef]
17. Edwards, J.K.; Pritchard, J.; Lu, L.; Piccinini, M.; Shaw, G.; Carley, A.F.; Morgan, D.J.; Kiely, C.J.; Hutchings, G.J. The direct synthesis of hydrogen peroxide using platinum-promoted gold-palladium catalysts. *Angew. Chem. Int. Ed.* **2014**, *53*, 2381–2384. [CrossRef] [PubMed]
18. Gu, X.; Lu, Z.-H.; Jiang, H.-L.; Akita, T.; Xu, Q. Synergistic catalysis of metal organic framework-immobilized AuPd nanoparticles in dehydrogenation of formic acid for chemical hydrogen storage. *J. Am. Chem. Soc.* **2011**, *133*, 11822–11825. [CrossRef] [PubMed]
19. Gudarzi, D.; Ratchananusorn, W.; Turunen, I.; Heinonen, M.; Salmi, T. Promotional effects of Au in Pd-Au bimetallic catalysts supported onactivated carbon cloth (ACC) for direct synthesis of $H_2O_2$ from $H_2$ and $O_2$. *Catal. Today* **2015**, *248*, 58–68. [CrossRef]
20. Hao, Y.; Hao, G.-P.; Guo, D.-C.; Guo, C.-Z.; Li, W.-C.; Li, M.-R.; Lu, A.-H. Bimetallic Au-Pd nanoparticles confined in tubular mesoporous carbon as highly selective and reusable benzyl alcohol oxidation catalysts. *ChemCatChem* **2012**, *4*, 1595–1602. [CrossRef]
21. Menegazzo, F.; Manzoli, M.; Signoretto, M.; Pinna, F.; Strukul, G. $H_2O_2$ direct synthesis under mild conditions on Pd-Au samples: Effectof the morphology and of the composition of the metallic phase. *Catal. Today* **2015**, *248*, 18–27. [CrossRef]
22. Belin, S.; Bracey, C.L.; Briois, V.; Ellis, P.R.; Hutchings, G.J.; Hyde, T.I.; Sankar, G. CuAu/$SiO_2$ catalysts for the selective oxidation of propene to acrolein: The impact of catalyst preparation variables on material structure and catalytic performance. *Catal. Sci. Technol.* **2013**, *3*, 2944–2957. [CrossRef]
23. Chimentao, R.J.; Medina, F.; Fierro, J.L.G.; Llorca, J.; Sueiras, J.E.; Cesteros, Y.; Salagre, P. Propene epoxidation by nitrous oxide over Au-Cu/$TiO_2$ alloy catalysts. *J. Mol. Catal. A* **2007**, *274*, 159–168. [CrossRef]
24. Guan, Y.; Hensen, E.J.M. Selective oxidation of ethanol to acetaldehyde by AuIr catalysts. *J. Catal.* **2013**, *305*, 135–145. [CrossRef]
25. Gallo, A.; Montini, T.; Marelli, M.; Minguzzi, A.; Gombac, V.; Psaro, R.; Fornasiero, P.; Santo, V.D. $H_2$ production by renewables photoreforming on Pt-Au/$TiO_2$ catalysts activated by reduction. *ChemSusChem* **2012**, *5*, 1800–1811. [CrossRef] [PubMed]
26. Na, H.; Zhu, T.; Liu, Z. Effect of preparation method on the performance of Pt-Au/$TiO_2$ catalysts for the catalytic co-oxidation of HCHO and CO. *Catal. Sci. Technol.* **2014**, *4*, 2051–2057. [CrossRef]

27. Chen, C.; Yang, H.; Chen, J.; Zhang, R.; Guo, L.; Gan, H.; Song, B.; Zhu, W.; Hua, L.; Hou, Z. One-pot tandem catalytic synthesis of α,β-unsaturated nitriles from alcohol with nitriles in aqueous phase. *Catal. Comm.* **2014**, *47*, 49–53. [CrossRef]
28. Haruta, M. Catalysis of gold nanoparticles deposited on metal oxides. *Cattech* **2002**, *6*, 102–115. [CrossRef]
29. Prati, L.; Martra, G. New gold catalysts for liquid phase oxidation. *Gold Bull.* **1999**, *32*. [CrossRef]
30. Mimura, N.; Hiyoshi, N.; Date, M.; Fujitani, T.; Dumeignil, F. Microscope analysis of Au-Pd/$TiO_2$ glycerol oxidation catalysts prepared by deposition—Precipitation method. *Catal. Lett.* **2014**, *144*, 2167–2175. [CrossRef]
31. Sasirekha, N.; Sangeetha, P.; Chen, Y.-W. Bimetallic Au-Ag/$CeO_2$ catalysts for preferential oxidation of CO in hydrogen-rich stream: Effect of calcination temperature. *J. Phys. Chem. C* **2014**, *118*, 15226–15233. [CrossRef]
32. La Parola, V.; Testa, M.L.; Venezia, A.M. Pd and PdAu catalysts supported over 3-MPTES grafted HMS used in the HDS of thiophene. *Appl. Catal. Environ.* **2012**, *119–120*, 248–255. [CrossRef]
33. Li, L.; Wang, C.; Ma, X.; Yang, Z.; Lu, X. An Au-Cu bimetal catalyst supported on mesoporous $TiO_2$ with stable catalytic performance in CO oxidation. *Chin. J. Catal.* **2012**, *33*, 1778–1782. [CrossRef]
34. Delannoy, L.; Thrimurthulu, G.; Reddy, P.S.; Méthivier, C.; Nelayah, J.; Reddy, B.M.; Ricolleau, C.; Louis, C. Selective hydrogenation of butadiene over $TiO_2$ supported copper, gold and gold-copper catalysts prepared by deposition precipitation. *Phys. Chem. Chem. Phys.* **2014**, *16*, 26514–26527. [CrossRef] [PubMed]
35. Aguilar-Tapia, A.; Zanella, R.; Calers, C.; Louis, C.; Delannoy, L. Synergistic effects of Ir-Au/$TiO_2$ catalysts in the total oxidation of propene: Influence of the activation conditions. *Phys. Chem. Chem. Phys.* **2015**, *17*, 28022–28032. [CrossRef] [PubMed]
36. Sandoval, A.; Delannoy, L.; Méthivier, C.; Louis, C.; Zanella, R. Synergetic effect in bimetallic Au-Ag/$TiO_2$ catalysts for CO oxidation: Insights from *in situ* characterization. *Phys. Chem. Chem. Phys.* **2015**, *17*, 28022–28032. [CrossRef]
37. Kittisakmontree, P.; Pongthawornsakun, B.; Yoshida, H.; Fujita, S.-I.; Arai, M.; Panpranot, J. The liquid-phase hydrogenation of 1-heptyne over Pd-Au/$TiO_2$ catalysts prepared by the combination of incipient wetness impregnation and deposition—Precipitation. *J. Catal.* **2013**, *297*, 155–164. [CrossRef]
38. Olmos, C.M.; Chinchilla, L.E.; Delgado, J.J.; Hungrıa, A.B.; Blanco, G.; Calvino, J.J.; Chen, X. CO oxidation over bimetallic Au-Pd supported on ceria-zirconia catalysts: Effects of oxidation temperature and Au:Pd molar ratio. *Catal. Lett.* **2016**, *146*, 144–156. [CrossRef]
39. Chinchilla, L.E.; Olmos, C.M.; Villa, L.; Carlsson, A.; Prati, L.; Chen, X.; Blanco, G.; Calvino, J.J.; Hungría, A.B. Ru-modified Au catalysts supported on ceria-zirconia for the selectiveoxidation of glycerol. *Catal. Today* **2015**, *253*, 178–189. [CrossRef]
40. Liao, X.; Chu, W.; Dai, X.; Pitchon, V. Bimetallic Au-Cu supported on ceria for PROX reaction: Effects of Cu/Au atomic ratios and thermal pretreatments. *Appl. Catal. Environ.* **2013**, *142–143*, 25–37. [CrossRef]
41. Liu, X.; Wang, A.; Wang, X.; Mou, C.-Y.; Zhang, T. Au-Cu alloy nanoparticles confined in SBA-15 as a highly efficient catalyst for CO oxidation. *Chem. Commun.* **2008**. [CrossRef] [PubMed]
42. Liu, X.; Wang, A.; Yang, X.; Zhang, T.; Mou, C.-Y.; Su, D.-S.; Li, J. Synthesis of thermally stable and highly active bimetallic Au-Ag nanoparticles on inert supports. *Chem. Mater.* **2009**, *21*, 410–418. [CrossRef]
43. Liu, X.; Wang, A.; Zhang, T.; Su, D.-S.; Mou, C.-Y. Au-Cu alloy nanoparticles supported on silica gel as catalyst for CO oxidation: Effects of Au/Cu ratios. *Catal. Today* **2011**, *160*, 103–108. [CrossRef]
44. Regan, M.R.; Banerjee, I.A. Preparation of Au-Pd bimetallic nanoparticles in porous germania nanospheres: A study of their morphology and catalytic activity. *Scr. Mater.* **2006**, *54*, 909–914. [CrossRef]
45. Bauer, J.C.; Mullins, D.; Li, M.; Wu, Z.; Payzant, E.A.; Overbury, S.H.; Dai, S. Synthesis of silica supported AuCu nanoparticle catalysts and the effects of pretreatment conditions for the CO oxidation reaction. *Phys. Chem. Chem. Phys.* **2011**, *13*, 2571–2581. [CrossRef] [PubMed]
46. Xiao, Q.; Liu, Z.; Bo, A.; Zavahir, S.; Sarina, S.; Bottle, S.; Riches, J.D.; Zhu, H. Catalytic transformation of aliphatic alcohols to corresponding esters in $O_2$ under neutral conditions using visible-light irradiation. *J. Am. Chem. Soc.* **2015**, *137*, 1956–1966. [CrossRef] [PubMed]
47. Yan, S.; Gao, L.; Zhang, S.; Gao, L.; Zhang, W.; Li, Y. Investigation of AuNi/C anode catalyst for direct methanol fuel cells. *Int. J. Hydr. Ener.* **2013**, *38*, 12838–12846. [CrossRef]
48. Qiao, P.; Zou, S.; Xu, S.; Liu, J.; Li, Y.; M, G.; Xiao, L.; Loua, H.; Fan, J. A general synthesis strategy of multi-metallic nanoparticles within mesoporous titania via *in situ* photo-deposition. *J. Mater. Chem. A* **2014**, *2*, 17321–17328. [CrossRef]

49. Tanaka, A.; Hashimoto, K.; Kominami, H. Gold and copper nanoparticles supported on cerium(IV) oxide—A photocatalyst mineralizing organic acids under red light irradiation. *ChemCatChem* **2011**, *3*, 1619–1623. [CrossRef]
50. Wu, T.; Ma, J.; Wang, X.; Liu, Y.; Xu, H.; Gao, J.; Wang, W.; Liu, Y.; Yan, J. Graphene oxide supported Au-Ag alloy nanoparticles with different shapes and their high catalytic activities. *Nanotechnology* **2013**, *24*, 125301. [CrossRef] [PubMed]
51. Chen, X.; Cai, Z.; Chen, X.; Oyama, M. AuPd bimetallic nanoparticles decorated on graphene nanosheets: Their green synthesis, growth mechanism and high catalytic ability in 4-nitrophenol reduction. *J. Mater. Chem. A* **2014**, *2*, 5668–5674. [CrossRef]
52. Villa, A.; Wang, D.; Veith, G.M.; Vindigni, F.; Prati, L. Sol immobilization technique: A delicate balance between activity, selectivity and stability for gold catalyst. *Catal. Sci. Technol.* **2013**, *3*, 3036–3041. [CrossRef]
53. Quintanilla, A.; Butselaar-Orthlieb, V.C.L.; Kwakernaak, C.; Sloof, W.G.; Kreutzer, M.T.; Kapteijn, F. Weakly bound capping agents on gold nanoparticles in catalysis: Surface poison? *J. Catal.* **2010**, *271*, 104–114. [CrossRef]
54. Zhong, Z.; Lin, J.; Teh, S.-P.; Teo, J.; Dautzenberg, F.M. A rapid and efficient method to deposit gold particles on catalyst supports and its application for CO oxidation at low temperatures. *Adv. Funct. Mater.* **2007**, *17*, 1402–1408. [CrossRef]
55. Menard, L.D.; Xu, F.; Nuzzo, R.G.; Yang, J.C. Preparation of $TiO_2$-supported Au nanoparticle catalysts from a Au13 cluster precursor: Ligand removal using ozone exposure *versus* a rapid thermal treatment. *J. Catal.* **2006**, *243*, 64–73. [CrossRef]
56. Llorca, J.; Casanovas, A.; Domınguez, M.; Casanova, I.; Angurell, I.; Seco, M.; Rossell, O. Plasma-activated core-shell gold nanoparticle films with enhanced catalytic properties. *J. Nano. Res.* **2008**, *10*, 537–542. [CrossRef]
57. Zhong, R.-Y.; Yan, X.-H.; Gao, Z.-K.; Zhang, R.-J.; Xu, B.-Q. Stabilizer substitution and its effect on the hydrogenation catalysis by Au nanoparticles from colloidal synthesis. *Catal. Sci. Technol.* **2013**, *3*, 3013–3019. [CrossRef]
58. Lopez-Sanchez, J.A.; Dimitratos, N.; Hammond, C.; Brett, G.L.; Kesavan, L.; White, S.; Miedziak, P.; Tiruvalam, R.; Jenkins, R.L.; Carley, A.F.; et al. Facile removal of stabilizer-ligands from supported gold nanoparticles. *Nat. Chem.* **2011**, *3*, 551–556. [CrossRef] [PubMed]
59. Gandarias, I.; Miedziak, P.J.; Nowicka, E.; Douthwaite, M.; Morgan, D.J.; Hutchings, G.J.; Taylor, S.H. Selective oxidation of *n*-butanol using gold-palladium supported nanoparticles under base-free conditions. *ChemSusChem* **2015**, *8*, 473–480. [CrossRef] [PubMed]
60. Luo, M.; Hong, Y.; Yao, W.; Huang, C.; Xu, Q.; Wu, Q. Facile removal of polyvinylpyrrolidone (PVP) adsorbates from Pt alloy nanoparticles. *J. Mater. Chem. A* **2015**, *3*, 2770–2775. [CrossRef]
61. Naresh, N.; Wasim, F.G.S.; Ladewig, B.P.; Neergat, M. Removal of surfactant and capping agent from Pd nanocubes (Pd-NCs) using tert-butylamine: Its effect on electrochemical characteristics. *J. Mater. Chem. A* **2013**, *1*, 8553–8559. [CrossRef]
62. Ansar, S.M.; Ameer, F.S.; Hu, W.; Zou, S.; Charles, U.; Pittman, J.; Zhang, D. Removal of molecular adsorbates on gold nanoparticles using sodium borohydride in water. *Nano Lett.* **2013**, *13*, 1226–1229. [CrossRef] [PubMed]
63. Zhao, Y.; Jia, L.; Medrano, J.A.; Ross, J.R.H.; Lefferts, L. Supported Pd catalysts prepared via colloidal method: The effect of acids. *ACS Catal.* **2013**, *3*, 2341–2352. [CrossRef]
64. Monzo, J.; Koper, M.T.M.; Rodriguez, P. Removing polyvinylpyrrolidone from catalytic Pt nanoparticles without modification of superficial order. *ChemPhysChem* **2012**, *13*, 709–715. [CrossRef] [PubMed]
65. Bianchi, C.L.; Canton, P.; Dimitratos, N.; Porta, F.; Prati, L. Selective oxidation of glycerol with oxygen using mono and bimetallic catalysts based on Au, Pd and Pt metals. *Catal. Today* **2005**, *102–103*, 203–212. [CrossRef]
66. Wang, D.; Villa, A.; Porta, F.; Su, D.; Prati, L. Single-phase bimetallic system for the selective oxidation of glycerol to glycerate. *Chem. Comm.* **2006**, 1956–1958. [CrossRef] [PubMed]
67. Wang, D.; Villa, A.; Prati, L.; Porta, F.; Su, D. Bimetallic gold/palladium catalysts: Correlation between nanostructure and synergistic effects. *J. Phys. Chem. C* **2008**, *112*, 8617–8622. [CrossRef]
68. Villa, A.; Wang, D.; Su, D.; Veith, G.M.; Prati, L. Using supported Au nanoparticles as starting material for preparing uniform Au/Pd bimetallic catalysts. *Phys. Chem. Chem. Phys.* **2010**, *12*, 2183–2189. [CrossRef] [PubMed]

69. Lopez-Sanchez, J.A.; Dimitratos, N.; Miedziak, P.; Ntainjua, E.; Edwards, J.K.; Morgan, D.; Carley, A.F.; Tiruvalam, R.; Kiely, C.J.; Hutchings, G.J. Au-Pd supported nanocrystals prepared by a sol immobilisation technique as catalysts for selective chemical synthesis. *Physi. Chem. Chem. Phys.* **2008**, *10*, 1921–1930. [CrossRef] [PubMed]
70. Konuspayeva, Z.; Afanasiev, P.; Nguyen, T.-S.; Felice, L.D.; Morfin, F.; Nguyen, N.-T.; Nelayah, J.; Ricolleau, C.; Li, Z.Y.; Yuan, J.; et al. Au–Rh and Au–Pd nanocatalysts supported on rutile titania nanorods: Structure and chemical stability. *Phys. Chem. Chem. Phys.* **2015**, *17*, 28112–28120. [CrossRef] [PubMed]
71. Benkó, T.; Beck, A.; Frey, K.; Srankó, D.F.; Geszti, O.; Sáfrán, G.; Maróti, B.; Schay, Z. Bimetallic Ag-Au/$SiO_2$ catalysts: Formation, structure and synergisticactivity in glucose oxidation. *Appl. Catal. A Gen.* **2014**, *479*, 103–111. [CrossRef]
72. Rodrigues, E.G.; Pereira, M.F.R.; Chen, X.; Delgado, J.J.; Órfão, J.J.M. Selective oxidation of glycerol over platinum-based catalysts supported on carbon nanotubes. *Ind. Eng. Chem. Res.* **2013**, *52*, 17390–17398. [CrossRef]
73. Venezia, A.M.; Liotta, L.F.; Pantaleo, G.; Parola, V.L.; Deganello, G.; Beck, A.; Koppány, Z.; Frey, K.; Horváth, D.; Guczi, L. Activity of $SiO_2$ supported gold-palladium catalysts in CO oxidation. *Appl. Catal. A* **2003**, *251*, 359–368. [CrossRef]
74. Marx, S.; Krumeich, F.; Baiker, A. Surface properties of supported, colloid-derived gold/palladium mono- and bimetallic nanoparticles. *J. Phys. Chem. C* **2011**, *115*, 8195–8205. [CrossRef]
75. Guczi, L.; Becka, A.; Horváth, A.; Koppány, Z.; Stefler, G.; Frey, K.; Sajó, I.; Geszti, O.; Bazin, D.; Lynch, J. AuPd bimetallic nanoparticles on $TiO_2$: XRD, TEM, *in situ* EXAFS studies and catalytic activity in CO oxidation. *J. Mol. Catal. A* **2003**, *204–205*, 545–552. [CrossRef]
76. Alshammari, A.; Kockritz, A.; Kalevaru, V.N.; Bagabas, A.; Martin, A. Potential of supported gold bimetallic catalysts for green synthesis of adipic acid from cyclohexane. *Top. Catal.* **2015**, *58*, 1069–1076. [CrossRef]
77. Chen, H.; Li, Y.; Zhang, F.; Zhang, G.; Fan, X. Graphene supported Au-Pd bimetallic nanoparticles with core-shell structures and superior peroxidase-like activities. *J. Mater. Chem.* **2011**, *21*, 17658–17661. [CrossRef]
78. Verbruggen, S.W.; Keulemans, M.; Filippousi, M.; Flahaut, D.; Tendeloo, G.V.; Lacombe, S.; Martens, J.A.; Lenaerts, S. Plasmonic gold-silver alloy on $TiO_2$ photocatalysts with tunablevisible light activity. *Appl. Catal. B Environ.* **2014**, *156–157*, 116–121. [CrossRef]
79. Llorca, J.; Domínguez, M.; Ledesma, C.; Chimentão, R.J.; Medina, F.; Sueiras, J.S.; Angurell, I.; Seco, M.; Rossell, O. Propene epoxidation over $TiO_2$-supported Au-Cu alloy catalysts prepared from thiol-capped nanoparticles. *J. Catal.* **2008**, *258*, 187–198. [CrossRef]
80. He, P.; Wang, Y.; Wang, X.; Pei, F.; Wang, H.; Liu, L.; Yi, L. Investigation of carbon supported Au-Ni bimetallic nanoparticles as electrocatalyst for direct borohydride fuel cell. *J. Power Sour.* **2011**, *196*, 1042–1047. [CrossRef]
81. He, P.; Wang, X.; Liu, Y.; Liu, X.; Yi, L. Comparison of electrocatalytic activity of carbon-supported Au-M (M [ Fe, Co, Ni, Cu and Zn) bimetallic nanoparticles for direct borohydride fuel cells. *Int. J. Hydr. Ener.* **2012**, *37*, 11984–11993. [CrossRef]
82. Szumełda, T.; Drelinkiewicz, A.; Kosydar, R.; Gurgul, J. Hydrogenation of cinnamaldehyde in the presence of PdAu/C catalystsprepared by the reverse "water-in-oil" microemulsion method. *Appl. Catal. A Gen.* **2014**, *487*, 1–15. [CrossRef]
83. Menezes, W.G.; Zielasek, V.; Thiel, K.; Hartwig, A.; Bäumer, M. Effects of particle size, composition, and support on catalytic activity of AuAg nanoparticles prepared in reverse block copolymer micelles as nanoreactors. *J. Catal.* **2013**, *299*, 222–231. [CrossRef]
84. Lee, L.-C.; Xiao, C.; Huang, W.; Zhao, Y. Palladium-gold bimetallic nanoparticle catalysts prepared by "controlled release" from metalloaded interfacially cross-linked reverse micelles. *New J. Chem.* **2015**, *39*, 2459–2466. [CrossRef]
85. Scott, R.W.J.; Wilson, O.M.; Crooks, R.M. Synthesis, characterization, and applications of dendrimer-encapsulated nanoparticles. *J. Phys. Chem. B* **2005**, *109*, 692–704. [CrossRef] [PubMed]
86. Chandler, B.D.; Gilbertson, J.D. PAMAM dendrimer templated nanoparticle catalysts. In *Nanoparticles and Catalysis*; Astruc, D., Ed.; Wiley-VCH: Weinheim, Germany, 2007.
87. Lang, H.; Maldonado, S.; Stevenson, K.J.; Chandler, B.D. Synthesis and characterization of dendrimer templated supported bimetallic Pt-Au nanoparticles. *J. Am. Chem. Soc.* **2004**, *126*, 12949–12956. [CrossRef] [PubMed]

88. Auten, B.J.; Lang, H.; Chandler, B.D. Dendrimer templates for heterogeneous catalysts: Bimetallic Pt-Au nanoparticles on oxide supports. *Appl. Catal. B* **2008**, *81*, 225–235. [CrossRef]
89. Chandler, B.D.; Long, C.G.; Gilbertson, J.D.; Pursell, C.J.; Vijayaraghavan, G.; Stevenson, K.J. Enhanced oxygen activation over supported bimetallic Au-Ni catalysts. *J. Phys. Chem. C* **2010**, *114*, 11498–11508. [CrossRef]
90. Song, Y.-J.; Jesús, Y.M.L.-D.; Fanson, P.T.; Williams, C.T. Preparation and characterization of dendrimer-derived bimetallic Ir-Au/$Al_2O_3$ catalysts for CO oxidation. *J. Phys. Chem. C* **2013**, *117*, 10999–11007. [CrossRef]
91. Zheng, Z.; Li, H.; Liu, T.; Cao, R. Monodisperse noble metal nanoparticles stabilized in SBA-15: Synthesis, characterization and application in microwave-assisted Suzuki-Miyaura coupling reaction. *J. Catal.* **2010**, *270*, 268–274. [CrossRef]
92. Pasini, T.; Piccinini, M.; Blosi, M.; Bonelli, R.; Albonetti, S.; Dimitratos, N.; Lopez-Sanchez, J.A.; Sankar, M.; He, Q.; Kiely, C.J.; et al. Selective oxidation of 5-hydroxymethyl-2-furfural using supported gold-copper nanoparticles. *Green Chem.* **2011**, *13*, 2091–2099. [CrossRef]
93. Yin, M.; Huang, Y.; Lv, Q.; Liang, L.; Liao, J.; Liu, C.; Xing, W. Improved direct electrooxidation of formic acid by increasing Au fraction on the surface of PtAu alloy catalyst with heat treatment. *Electrochim. Acta* **2011**, *58*, 6–11. [CrossRef]
94. Tang, S.; Vongehr, S.; Meng, X. Controllable incorporation of Ag and Ag-Au nanoparticles in carbon spheres for tunable optical and catalytic properties. *J. Mater. Chem.* **2010**, *20*, 5436–5445. [CrossRef]
95. Tang, S.; Vongehr, S.; He, G.; Chen, L.; Meng, X. Highly catalytic spherical carbon nanocomposites allowing tunable activity via controllable Au-Pd doping. *J. Coll. Interf. Sci.* **2012**, *375*, 125–133. [CrossRef] [PubMed]
96. Chandler, B.D.; Schabel, A.B.; Blanford, C.F.; Pignolet, L.H. Preparation and characterization of supported bimetallic Pt-Au particle catalysts from molecular cluster and chloride salt precursors. *J. Catal.* **1999**, *187*, 367–384. [CrossRef]
97. Albonetti, S.; Bonelli, R.; Delaigle, R.; Femoni, C.; Gaigneaux, E.M.; Morandi, V.; Ortolani, L.; Tiozzo, C.; Zacchini, S.; Trifiro, F. Catalytic combustion of toluene over cluster-derived gold/iron catalysts. *Appl. Catal. A Gen.* **2010**, *372*, 138–146. [CrossRef]
98. Redjala, T.; Remita, H.; Apostolescu, G.; Mostafavi, M.; Thomazeau, C.; Uzio, D. Bimetallic Au-Pd and Ag-Pd clusters synthesised by $\gamma$ or electron beam radiolysis and study of the reactivity/structure relationships in the selective hydrogenation of buta-1,3-diene. *Oil Gas Sci. Tech. Rev. IFP* **2006**, *61*, 789–797. [CrossRef]
99. Doherty, R.P.; Krafft, J.-M.; Méthivier, C.; Casale, S.; Remita, H.; Louis, C.; Thomas, C. On the promoting effect of Au on CO oxidation kinetics of Au-Pt bimetallic nanoparticles supported on $SiO_2$: An electronic effect? *J. Catal.* **2012**, *287*, 102–113. [CrossRef]
100. Yamamoto, T.A.; Nakagawa, T.; Seino, S.; Nitani, H. Bimetallic nanoparticles of PtM (M = Au, Cu, Ni) supported on iron oxide: Radiolytic synthesis and CO oxidation catalysis. *Appl. Catal. A* **2010**, *387*, 195–202. [CrossRef]
101. Barbier, J. *Handbook of Heterogeneous Catalysis*; Ertl, G., Knözinger, H., Weitkamp, J., Eds.; Wiley VCH: Weinheim, Germany, 1997; p. 257.
102. Epron, F.; Especel, C.; Lafaye, G.; Marécot, P. Multimetallic nanoparticles prepared by redox processes applied in catalysis. In *Nanoparticles and Catalysis*; Astruc, D., Ed.; Wiley VCH: Weinheim, Germany, 2007; pp. 281–304.
103. Especel, C.; Duprez, D.; Epron, F. Bimetallic catalysts for hydrogenation in liquid phase. *C. R. Chim.* **2014**, *17*, 790–800. [CrossRef]
104. Beard, K.D.; Schaal, M.T.; Zee, J.W.V.; Monnier, J.R. Preparation of highly dispersed PEM fuel cell catalysts using electroless deposition methods. *Appl. Catal. B Environ.* **2007**, *72*, 262–271. [CrossRef]
105. Rebelli, J.; Rodriguez, A.A.; Ma, S.; Williams, C.T.; Monnier, J.R. Preparation and characterization of silica-supported, group IB-Pd bimetallic catalysts prepared by electroless deposition methods. *Catal. Today* **2011**, *160*, 170–178. [CrossRef]
106. An, Q.; Yu, M.; Zhang, Y.; Ma, W.; Guo, J.; Wang, C. $Fe_3O_4$ carbon microsphere supported Ag-Au bimetallic nanocrystals with the enhanced catalytic activity and selectivity for the reduction of nitroaromatic compounds. *J. Phys. Chem. C* **2012**, *116*, 22432–22440. [CrossRef]
107. Guan, Y.; Zhao, N.; Tang, B.; Jia, Q.; Xu, X.; Liu, H.; Boughton, R.I. A stable bimetallic Au-Ag/$TiO_2$ nanopaper for aerobic oxidation of benzyl alcohol. *Chem. Comm.* **2013**, *49*, 11524–11526. [CrossRef] [PubMed]

108. Jia, Q.; Zhao, D.; Tang, B.; Zhao, N.; Li, H.; Sang, Y.; Bao, N.; Zhang, X.; Xu, X.; Liu, H. Synergistic catalysis of Au-Cu/$TiO_2$-NB nanopaper in aerobic oxidation of benzyl alcohol. *J. Mater. Chem. A* **2014**, *2*, 16292–16298. [CrossRef]
109. Sarkany, A.; Horvath, À.; Beck, A. Hydrogenation of acetylene over low loaded Pd and Pd-Au/$SiO_2$ catalysts. *Appl. Catal. A Gen.* **2002**, *229*, 117–125. [CrossRef]
110. Choudhary, T.V.; Sivadinarayana, C.; Datye, A.K.; Kumar, D.; Goodman, D.W. Acetylene hydrogenation on Au-based catalysts. *Catal. Lett.* **2003**, *86*, 1–8. [CrossRef]
111. Espinosa, G.; Angel, G.D.; Barbier, J.; Marécot, P.; Schifter, I. Preparation of alumina-supported palladium platinum catalysts by surface redox reactions. Activity for complete hydrocarbon oxidation. *Stud. Surf. Sci. Catal.* **1997**, *111*, 421–426.
112. Maris, E.P.; Ketchie, W.C.; Murayama, M.; Davis, R.J. Glycerol hydrogenolysis on carbon-supported PtRu and AuRu bimetallic catalysts. *J. Catal.* **2007**, *251*, 281–294. [CrossRef]
113. Rebelli, J.; Detwiler, M.; Ma, S.; Williams, C.T.; Monnier, J.R. Synthesis and characterization of Au-Pd/$SiO_2$ bimetallic catalysts prepared by electroless deposition. *J. Catal.* **2010**, *270*, 224–233. [CrossRef]
114. Alba-Rubio, A.C.; Plauck, A.; Stangland, E.E.; Mavrikakis, M.; Dumesic, J.A. Direct synthesis of hydrogen peroxide over Au-Pd catalysts prepared by electroless deposition. *Catal. Lett.* **2015**, *145*, 2057–2065. [CrossRef]
115. Griffin, M.B.; Rodriguez, A.A.; Montemore, M.M.; Monnier, J.R.; Williams, C.T.; Medlin, J.W. The selective oxidation of ethylene glycol and 1,2-propanediol on Au, Pd, and Au-Pd bimetallic catalysts. *J. Catal.* **2013**, *307*, 111–120. [CrossRef]
116. Monyanon, S.; Pongstabodee, S.; Luengnaruemitchai, A. Preferential oxidation of carbon monoxide over Pt, Au monometallic catalyst, and Pt-Au bimetallic catalyst supported on ceria in hydrogen-rich reformate. *J. Chin. Inst. Chem. Eng.* **2007**, *38*, 435–441. [CrossRef]
117. Pramanik, S.; Mishra, M.K.; De, G. Crystal structure tailoring of Au-Cu alloy NPs using the embedding film matrix as template. *Cryst. Eng. Comm.* **2014**, *16*, 56–63. [CrossRef]
118. Bönnemann, H.; Endruschat, U.; Tesche, B.; Rufınska, A.; Lehmann, C.W.; Wagner, F.E.; Filoti, G.; Parvulescu, V.; Parvulescu, V.I. An $SiO_2$-embedded nanoscopic Pd/Au alloy colloid. *Eur. J. Inorg. Chem.* **2000**, *12*, 819–822. [CrossRef]
119. Dash, P.; Bond, T.; Fowler, C.; Hou, W.; Coombs, N.; Scott, R.W.J. Rational design of supported PdAu nanoparticle catalysts from structured nanoparticle precursors. *J. Phys. Chem. C* **2009**, *113*, 12719–12730. [CrossRef]
120. Jiang, H.-L.; Umegaki, T.; Akita, T.; Zhang, X.-B.; Haruta, M.; Xu, Q. Bimetallic Au-Ni nanoparticles embedded in $SiO_2$ Nanospheres: Synergetic catalysis in hydrolytic dehydrogenation of ammonia borane. *Chem. Eur. J.* **2010**, *16*, 3132–3137. [CrossRef] [PubMed]
121. Scott, R.W.J.; Sivadinarayana, C.; Wilson, O.M.; Yan, Z.; Goodman, D.W.; Crooks, R.M. Titania-supported PdAu bimetallic catalysts prepared from dendrimer-encapsulated nanoparticle precursors. *J. Am. Chem. Soc.* **2005**, *127*, 1380–1381. [CrossRef] [PubMed]
122. Chen, Y.; Lim, H.; Tang, Q.; Gao, Y.; Sun, T.; Yan, Q.; Yang, Y. Solvent-free aerobic oxidation of benzyl alcohol over Pd monometallic and Au-Pd bimetallic catalysts supported on SBA-16 mesoporous molecular sieves. *Appl. Catal. A* **2010**, *380*, 55–65. [CrossRef]
123. Zheng, J.; Lin, H.; Wang, Y.; Zheng, X.; Duan, X.; Yuan, Y. Efficient low-temperature selective hydrogenation of esters on bimetallic Au-Ag/SBA-15 catalyst. *J. Catal.* **2013**, *297*, 110–118. [CrossRef]
124. Lin, H.; Zheng, J.; Zheng, X.; Gu, Z.; Yuan, Y.; Yang, Y. Improved chemoselective hydrogenation of crotonaldehyde over bimetallic AuAg/SBA-15 catalyst. *J. Catal.* **2015**, *330*, 135–144. [CrossRef]
125. Qu, Z.; Ke, G.; Wang, Y.; Liu, M.; Jiang, T.; Gao, J. Investigation of factors influencing the catalytic performance of CO oxidation over Au-Ag/SBA-15 catalyst. *Appl. Surf. Sci.* **2013**, *277*, 293–301. [CrossRef]
126. Sobczak, I.; Dembowiak, E. The effect of AuAg-MCF and AuAg-NbMCF catalysts pretreatment onthe gold-silver alloy formation and the catalytic behavior in selectivemethanol oxidation with oxygen. *J. Mol. Catal. A* **2015**, *409*, 137–148. [CrossRef]
127. Jiang, H.-L.; Akita, T.; Ishida, T.; Haruta, M.; Xu, Q. Synergistic catalysis of Au@Ag core-shell nanoparticles stabilized on metal-organic framework. *J. Am. Chem. Soc.* **2011**, *133*, 1304–1306. [CrossRef] [PubMed]
128. Long, J.; Liu, H.; Wu, S.; Liao, S.; Li, Y. Selective oxidation of saturated hydrocarbons using Au-Pd alloy nanoparticles supported on metal-organic frameworks. *ACS Catal.* **2013**, *3*, 667–654. [CrossRef]

129. Zhu, Q.-L.; Li, J.; Xu, Q. Immobilizing metal nanoparticles to metal-organic frameworks with size and location control for optimizing catalytic performance. *J. Am. Chem. Soc.* **2013**, *135*, 10210–10213. [CrossRef] [PubMed]
130. Li, J.; Zhua, Q.-L.; Xu, Q. Highly active AuCo alloy nanoparticles encapsulated in the pores of metal–organic frameworks for hydrolytic dehydrogenation of ammonia borane. *Chem. Comm.* **2014**, *50*, 5899–5901. [CrossRef] [PubMed]
131. Liu, Y.; Jia, S.-Y.; Wu, S.-H.; Li, P.-L.; Liu, C.-J.; Xu, Y.-M.; Qin, F.-X. Synthesis of highly dispersed metallic nanoparticles inside the pores of MIL-101(Cr) via the new double solvent method. *Catal. Commun.* **2015**, *70*, 44–48.